CHALMERS

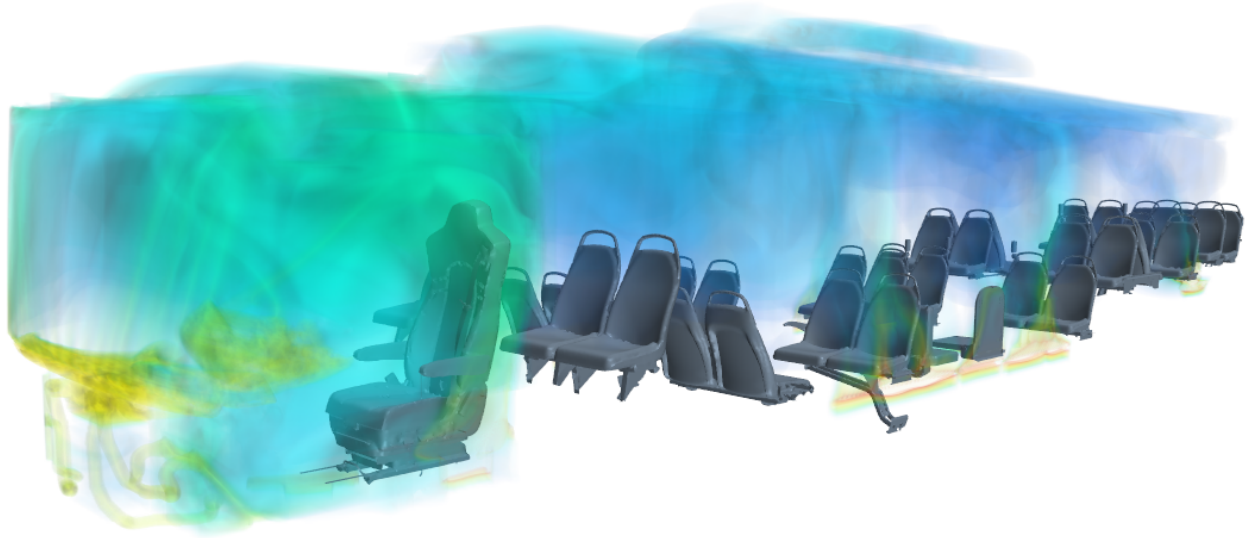

Unsteady Interior Climate Simulation of Electric Buses

Master's thesis in Applied Mechanics

NITHIN BHARADWAJ RAVINDRA

Department of Mechanics and Maritime Sciences
CHALMERS UNIVERSITY OF TECHNOLOGY
Göteborg, Sweden 2020

MASTER'S THESIS IN APPLIED MECHANICS

Unsteady Interior Climate Simulation of Electric Buses

NITHIN BHARADWAJ RAVINDRA

Department of Mechanics and Maritime Sciences
Division of Vehicle Engineering and Autonomous Systems
CHALMERS UNIVERSITY OF TECHNOLOGY

Göteborg, Sweden 2020

Unsteady Interior Climate Simulation of Electric Buses
NITHIN BHARADWAJ RAVINDRA

Master's thesis 2020:40
Department of Mechanics and Maritime Sciences
Division of Vehicle Engineering and Autonomous Systems
Chalmers University of Technology
SE-412 96 Göteborg
Sweden
Telephone: +46 (0)31-772 1000

Cover:
Volume render of temperature distribution in the cabin

Chalmers Reproservice
Göteborg, Sweden 2020

Unsteady Interior Climate Simulation of Electric Buses
Master's thesis in Applied Mechanics
NITHIN BHARADWAJ RAVINDRA
Department of Mechanics and Maritime Sciences
Division of Vehicle Engineering and Autonomous Systems
Chalmers University of Technology

Abstract

In today's world buses are one of the most popular means of transport for commuters in an urban setting. To maintain the thermal comfort of passengers inside the bus the heating, ventilation and air condition (HVAC) systems are used. These systems consume a large part of the total power consumption in the bus especially when working in extreme weather conditions. In urban areas, the energy lost to the external atmosphere is not only through the walls of the bus but also when the doors are opened for passengers to board or depart. The recent shift towards electrification of buses, especially in cities, makes analysing and reducing the power consumption of HVAC system ever so important.

This study uses Computational Fluid Dynamics(CFD) to frame a methodology for simulating the interior climate of bus. Simulations offer a way to test various cases at relatively lower cost and faster rate when compared to experiments. In this study initially a steady state model is built using Reynolds Averaged Navier Stokes(RANS) equations and realizable $k-\epsilon$ turbulence model with all the necessary HVAC system boundary conditions. The model is calibrated against the experiments by sweeping a scaling factor to find the heat transfer coefficient(HTC) of the exterior parts of the bus such as floor, roof, windows, walls etc. The calibrated model is then converted into an unsteady model using steady state simulation results as an initial solution. The unsteady model is built to simulate one standard door opening cycle, i.e, 20 seconds of opened door followed by 2 minutes of closed door simulation. The motion of the doors in the simulation is obtained by using overset mesh methodology. The model is built with one extreme weather condition of -8.3°C. The results from steady state describing the flow behaviour of the interior climate and the effect of door opening cycle on the interior climate from unsteady simulation are discussed in this study.

Keywords: Interior Climate, HVAC, CFD, Overset mesh, Electric bus, Unsteady simulation

Preface

This study has been done as a part of master thesis work for the Applied Mechanics master program at Chalmers University of Technology. This work was carried out at Volvo Bus Corporation under the supervision of Raman Yazdani(Lead engineer). This thesis is examined by Alexey Vdovin(Post Doctoral Researcher at department of Mechanics and Maritime Sciences in Chalmers University of Technology).

Acknowledgements

I would like to thank my supervisor at Volvo buses, Raman Yazdani, for his continued support and encouragement throughout the project. I would also like to thank Siemens for their support in software related queries. I would like to thank everyone at Virtual Verification & Analysis department for making me feel welcome and for having fruitful discussions regarding thesis work. I would like to also thank Alexey Vdovin for his guidance and for being my examiner.

Nomenclature

- ρ Density kg/m^3
- t Time s
- v_i Velocity in i-direction m/s
- x_i Location in i-direction m
- σ_{ji} Stress tensor kg/ms^2
- f_i Body forces N/m^3
- P Pressure kg/ms^2
- μ Dynamic viscosity N/m^2s
- S_{ij} Strain rate tensor s^-1
- T Temperature $^\circ C$
- k Thermal Conductivity W/mK
- z Net radiative heat source J/kgs
- l Turbulent length scale m
- ν_t Turbulent viscosity m^2/s
- Q Amount of heat transfer W
- $\dot{m}$ Mass flow rate kg/s
- c_p Specific heat constant J/kgK
- q_x Conductive heat flux W/m^2
- $q_{convective}$ Convective heat flux W/m^2
- h Convective heat transfer coefficient W/m^2K
- q_{rad} Heat flux due to radiation W/m^2
- ϵ Emissivity
- σ_b Stefan-Boltzmann constant W/m^2K^4
- δP Pressure drop kg/ms^2
- L Length of the porous media m
- P_i Inertial resistance kg/m^4
- P_v Viscous resistance kg/m^3s
- v Velocity m/s
- U Overall heat transfer coefficient W/m^2K
- A Cross sectional area to the heat flow m^2

Abstract i

Preface iii

Acknowledgements iii

Nomenclature v

1 Introduction 1
1.1 Background . . . 1
1.2 Literature Study . . . 1
1.3 Problem Definition . . . 2
1.4 Limitations . . . 2

2 Theory 3
2.1 Governing Equations . . . 3
2.1.1 Continuity Equation . . . 3
2.1.2 Momentum Equation . . . 3
2.1.3 Energy Equation . . . 4
2.2 Turbulence . . . 4
2.3 Heat Transfer . . . 5
2.3.1 Conduction . . . 5
2.3.2 Convection . . . 5
2.3.3 Radiation . . . 5
2.4 Components of HVAC system . . . 6

3 Method 9
3.1 Steady State Modelling . . . 9
3.1.1 Geometry . . . 9
3.1.2 Mesh . . . 9
3.1.2.1 Surface Wrapper . . . 10
3.1.2.2 Automated Volume Mesh . . . 12
3.1.3 Physics and Solver . . . 14
3.1.3.1 Physics . . . 14
3.1.3.2 Solver . . . 16
3.1.4 Boundary Conditions . . . 16
3.1.4.1 Roof Top Air Conditioning Unit . . . 16
3.1.4.2 Defroster . . . 18
3.1.4.3 Convectors and Heaters . . . 20
3.1.4.4 Convection . . . 20
3.1.5 Experimental Data . . . 21
3.1.6 Calibration . . . 21
3.2 Unsteady Model . . . 22
3.2.1 Geometry . . . 22
3.2.2 Mesh . . . 22
3.2.3 Physics and Solver . . . 24
3.2.4 Boundary Conditions . . . 24

4 Results 27
4.1 Simplified Model . . . 27
4.2 Steady State Model . . . 27
4.2.1 Calibration sweep . . . 28
4.2.2 Convergence . . . 30
4.2.3 Flow field . . . 32
4.2.4 Temperature distribution . . . 33
4.2.5 Boundary Heat Flux . . . 34
4.3 Unsteady Model . . . 36

5 Conclusions **47**

Bibliography **49**

1

Introduction

1.1 Background

Today people spend on an average 7% of time commuting everyday[1] and buses are one of the most popular means of transport in an urban setting. The heating, ventilation and air conditioning (HVAC) systems are used in these buses to maintain required amount of thermal comfort for passengers inside the bus. These systems consume a large amount of power while heating up or cooling down the cabin in extreme weather conditions[2]. In recent years, shift towards electrification of mobility can be observed and reducing the amount of power consumption of the HVAC system becomes ever so important.

In an urban setting, energy losses are not only through the exterior parts of the bus but also through opening of the doors during the boarding and departure of passengers. Temperature gradients increase inside the cabin when the doors are opened. The HVAC system would consume more energy to work against these gradients and achieve the required thermal comfort inside the cabin. Hence it becomes important to analyse the temperature and velocity distribution inside the bus before, during and after opening the door to see how loses in energy could be reduced.

Experimental analysis is reliable but expensive and takes more time to test all the cases that are required to understand the problem at hand. Computational Fluid Dynamics(CFD) simulations offer an alternative to this problem by solving the fluid flow using numerical methods. The current study is focused on one such simulation methodology for the interior climate of a city bus which is verified using the experimental data.

1.2 Literature Study

There have been many studies made on the interior climate of the vehicles both by using experiments and simulations.

One of the studies made by Zhang et al.[3][4] on a section of passenger compartment showed that the outside temperature has appreciable effect on the cooling load, hence on the energy consumption. It was also concluded that better flow circulation near the compartment bottom is favorable to improve the uniformity of temperature field around the driver's foot. Mike Liebers et al.[5] made an experimental investigation on the reduction of heat losses in the door opening of urban buses by using air-walls located on top of the door. This solution was found to be beneficial in reducing the energy losses when the doors were opened for longer duration. Roberto de Lieto Vollaro[6] studied the indoor climate in the city buses by using numerical simulation which was experimental validated. It was found that air screened doors can be used to get the same comfort level with a reduced indoor room temperature at two different locations in the bus. Ozgur Ekici[7] made a numerical analysis of heating in a section of coach bus cabin under transient state conditions. He found that predictions made by the numerical model was in good agreement with the experimental values. It was suggested to model whole bus passenger compartment to obtain closer values to experiments.

There have been publications regarding air distribution in other vehicles as well. Christian Suarez et al.[8] did CFD analysis of air distribution in a railway vehicle equipped with HVAC system. In this study it was found that there are larger temperature gradients inside the passenger compartment during winter conditions when compared to summer climate conditions. Ryan K. Dygert et al.[9] showed significant improvements of cross-contamination in their numerical model of aircraft cabin by introducing localised exhausts.

A study was made to develop an interior climate simulation methodology in steady state for three different weather conditions by EE Johansson and M Skärby[10]. In the present work, the steady state model is developed further to make it more realistic and calibrated with the experimental results. This model is then used to analyse the air flow and temperature inside the bus during a door opening cycle with an aim of using energy efficiently.

1.3 Problem Definition

The current study is focused on answering the following questions

- Steady state simulation methodology
  - What components of the bus have to be considered for steady state interior climate simulations?
  - What should be the mesh strategy for interior climate simulations?
  - What boundary conditions should be given to simulate the interior climate as accurately as possible?
  - What settings should be chosen for the numerical model and solver in order to simulate the interior climate?
- Unsteady simulation methodology
  - What time step should be chosen for simulating the unsteady interior climate simulation?
  - How does the boundary conditions change with respect to time?
- Door opening cycle
  - What strategy should be used to open the doors of the bus in the interior climate simulation?
  - What are the effects of door opening on interior climate?

1.4 Limitations

There are some simplifications made to the model in order to simulate the interior climate of city bus.

- All heat exchangers are treated as single stream heat exchangers. Coolant side of the heat exchanger is not considered.
- Condenser unit is not modelled inside the roof unit which is where the coolant is cooled.
- Fans are modelled using fan performance curves.
- No passengers are included in the simulations as the numerical model is calibrated using experiments which also do not include any passengers.
- Only temperature and air flow are analysed. Passenger and driver thermal comfort is not evaluated.
- Solar radiation effects can be neglected as the experiments are conducted in a closed room. Radiative heat transfer is also not considered as in an earlier study on interior climate it was shown that radiation effects were minimal for the ambient temperature considered in this thesis [10].

These simplifications are made due to availability of time, resources and ease of working. Limited computer resources increase the amount of time required for processes and this will limit the number of configurations that can be tested.

2

Theory

2.1 Governing Equations

Computational Fluid Dynamics(CFD) is the analysis of systems involving fluid flow and heat transfer using a computer-based simulation. This is done by solving governing equations of fluid flow numerically for a set of boundary conditions. The equations that govern the mechanics of fluid flow are Continuity Equation, Momentum Equation and Energy Equation.

2.1.1 Continuity Equation

The equation of continuity is mass balance of a fluid flowing in a volume. It is given by

$$\frac{d\rho}{dt} + \rho\frac{\partial v_i}{\partial x_i} = 0 \tag{2.1}$$

where ρ is the density of working fluid, v_i is the velocity in i-direction, t is the time and x_i is the location in the i-direction.

If the flow is considered to be incompressible, then density is a constant. Equation 2.1 can be re-written as

$$\frac{\partial v_i}{\partial x_i} = 0 \tag{2.2}$$

2.1.2 Momentum Equation

The momentum equation is the result of the Newton's second law of motion which states that rate of change in linear momentum of a fluid particle is directly proportional to the sum of forces acting on it.

$$\rho\frac{dv_i}{dt} = \frac{d\sigma_{ji}}{dx_j} + \rho f_i \tag{2.3}$$

where the first and second terms on right side represent the net force due to surface and volume forces respectively. σ_{ji} is the stress tensor and f_i is the body force.

For Newtonian viscous fluids, σ_{ji} is given by

$$\begin{aligned} \sigma_{ji} &= -P\delta_{ij} + 2\mu S_{ij} - \frac{2}{3}\mu S_{kk}\delta_{ij} \\ \tau_{ij} &= 2\mu S_{ij} - \frac{2}{3}\mu S_{kk}\delta_{ij} \end{aligned} \tag{2.4}$$

where P is the pressure, μ is the dynamic viscosity of the fluid, S_{ij} is a strain-rate tensor and δ_{ij} is the identity tensor. S_{ij} is given by,

$$S_{ij} = \frac{1}{2}(\frac{\partial v_i}{\partial x_j} + \frac{\partial v_j}{\partial x_i}) \tag{2.5}$$

Inserting equation 2.4 in 2.3 we get,

$$\rho\frac{dv_i}{dt} = -\frac{\partial P}{\partial x_i} + \frac{\partial}{\partial x_j}(2\mu S_{ij} - \frac{2}{3}\mu\frac{\partial v_k}{\partial x_k}\delta_{ij}) + \rho f_i \tag{2.6}$$

For incompressible flow and constant μ equation 2.6 can be re-written as

$$\rho\frac{dv_i}{dt} = -\frac{\partial P}{\partial x_i} + \mu\frac{\partial^2 v_i}{\partial x_j \partial x_j} + \rho f_i \tag{2.7}$$

2.1.3 Energy Equation

The first law of thermodynamics applies the conservation of energy to a system where there the energy is transferred in and out of the system. It states that net change in internal energy of the system is equal to the sum of net heat transfer into the system and net work done on the system. Energy equation, derived from the first law of thermodynamics, for a compressible flow is given by,

$$\rho c_p\frac{dT}{dt} = \Phi + \frac{\partial}{\partial x_i}(k\frac{\partial T}{\partial x_i}) + \rho z \tag{2.8}$$

where c_p is the specific heat constant, T is the temperature, k is the heat conductivity constant and z is the net radiative heat source.

The left hand side of the term denotes internal energy of the system. The first term on the right hand side of the equation denotes viscous dissipation. Viscous dissipation refers to irreversible viscous heating which is conversion of kinetic energy to thermal energy. The second term on the right hand side denotes the heat flux and the last term represents heat flux due to radiation.[10][11]

2.2 Turbulence

The chaotic and irregular characteristic of air is referred as turbulent flow. Air inside the cabin of the bus is turbulent and this is modelled using Realizable Two layer k-ϵ model in this study. k-ϵ model is a two equation model that solves transport equations for turbulent kinetic energy k and turbulent dissipation rate ϵ which are used to determine turbulent length scale and turbulent viscosity of the fluid. Turbulent length scale is given by,

$$l = \frac{k^{\frac{3}{2}}}{\epsilon} \tag{2.9}$$

Turbulent viscosity is given by,

$$\nu_t = c_\mu k^{\frac{1}{2}} l \tag{2.10}$$

Realizability refers to the mathematically constraint that all normal stresses should stay positive. This constraint can sometimes be violated in the standard $k-\epsilon$ model. This is overcome in the realizable $k-\epsilon$ model by solving an additional transport equation for the turbulent dissipation rate ϵ and by damping the coefficient c_μ using a function of mean flow and turbulent properties.

The term two layer in the model refers to an approach where the computation is divided into two layers. Turbulent dissipation rate ϵ and the turbulent viscosity ν_t are modelled as functions of wall distance in the cells close to the wall. Turbulent kinetic energy k is calculated across the entire domain. The values calculated close to the wall are blended smoothly with the values that are calculated far from wall.[12]

2.3 Heat Transfer

Zeroth law of thermodynamics describes thermal equilibrium in which two bodies initially at different temperatures when come in contact eventually attain same temperature. During this process of thermal equilibrium there is transfer of heat energy from one body to another. The amount of the heat transferred from one body to another is directly proportional to the difference in temperature, which is given by

$$Q = \dot{m} c_p \Delta T \tag{2.11}$$

where Q is the amount of heat transfer, $\dot{m}$ is the mass flow rate of the fluid, c_p is the specific heat constant for the material, ΔT is the temperature difference between body and the fluid. This process of heat transfer takes place in three different modes: Conduction, convection and radiation.

2.3.1 Conduction

Conduction is a mode of heat transfer that describes the transfer of energy either within the solid body or from one solid body to another body which is in direct contact with the first. The transfer of energy takes place due to molecular collisions where there is exchange of heat energy from high kinetic energy molecules to low kinetic energy molecules. Fourier's law states that the heat flux resulting from conductive heat transfer is directly proportional to magnitude of the temperature gradient. Fourier's law in one dimensional form can be expressed as,

$$q_x = -k \frac{dT}{dx} \tag{2.12}$$

where q_x is the heat flux due to conductive heat transfer, k is the thermal conductivity constant and T is the temperature.

2.3.2 Convection

Convection is a mode of heat transfer that describes the transfer of energy between fluid and solid surface. The transfer of energy takes place due to the bulk movement of fluid. Newton's law states that the rate of heat loss due to convection is directly proportional to the difference in temperature of the body and its surroundings. This can be expressed as,

$$q_{convective} = h(T_f - T_b) \tag{2.13}$$

where $q_{convective}$ is the convective heat flux, h is the heat transfer coefficient, T_f is the fluid temperature and T_b is the temperature of the body.

Convection could be of two types, natural and forced. In natural convection the motion of fluid is due the buoyancy forces that result from differences in density. The differences in temperature causes the changes in density of fluid where denser(heavier) part sinks and lighter part rises up leading to the bulk movement of the fluid. In forced convection the motion of fluid is due to an external source like a fan. It is generally used to enhance the rate of heat transfer.

2.3.3 Radiation

Radiation is a mode of heat transfer that describes the transfer of heat energy in the form of electromagnetic waves. Unlike conduction and convection, radiation does not require any material medium or any physical contact to transfer energy. Stefan Boltzmann's law states that the rate of heat transfer in a black body is directly proportional to the fourth power of the temperature of the body.

$$q_{rad} = \epsilon \sigma_b T^4 \tag{2.14}$$

where q_{rad} is the heat flux due to radiation, ϵ is emissivity of the body, σ_b is the Stefan-Boltzmann constant and T is the temperature of the body.

2.4 Components of HVAC system

The heating, ventilation and air conditioning (HVAC) system is used in buses to control the interior climate of the buses for the comfort of driver and passengers. The operation of the system depends on the outdoor temperature, i.e. heating air in cold ambient conditions and cooling air in hot and humid environments. The main components of the HVAC system are the roof top air conditioning unit, convectors, heaters and defroster. Figure 2.1 shows the position of these components inside the bus.

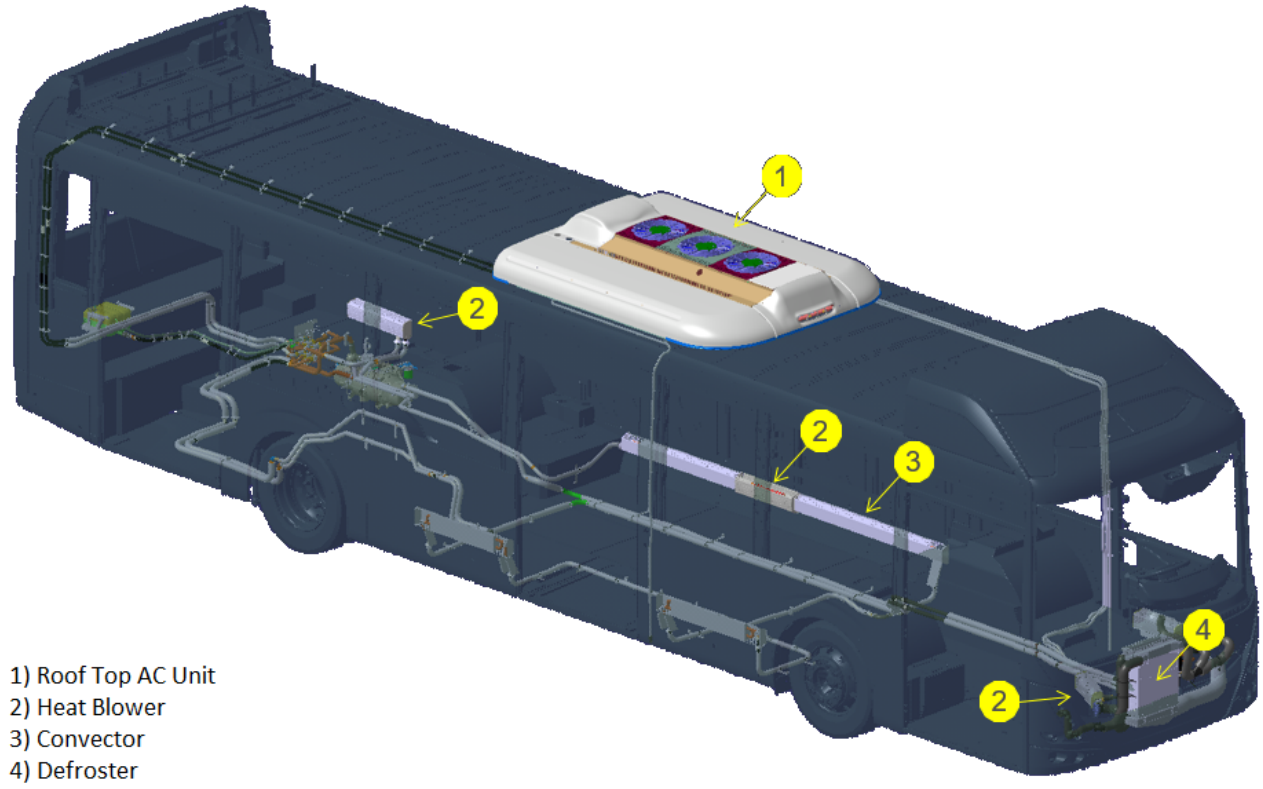

Figure 2.1: *Components of HVAC system*

Roof top AC unit removes heat from the bus using evaporator in the cooling mode. The cooled air is recirculated in the bus by forced convection with the help of blowers. This unit is also equipped with a heat pump which is used to heat the air going into the cabin in the heating mode. Heat pump and the evaporator works well for a particular range of temperature beyond which its efficiency is reduced. Figure 2.2 shows a cross section of the roof unit. The arrows at the bottom represent the air coming from the cabin to the roof unit which is cooled/heated and pushed back into the cabin by the blowers. The arrows at the top represent fresh air coming from outside through a flap which is not used in a city bus. The small arrows on top represent the air taken by the system to cool the coolant in a condenser.

Convectors transmit heat energy from hot water to surrounding air. These convectors use heat exchangers which increase the surface area which in turn increases the amount of heat transfer. Heat blower has the same functionality as that of the convector but uses a blower to increase the spread of heat by forced convection.

Defroster is used to defog or clean the windshield of the bus and control the climate around the driver. It consists of a heat exchanger, evaporator, air filter and a blower. Heat exchanger and evaporator is used in heating and cooling modes respectively which are shown in the figure 2.3. There are multiple outlets going from the defroster one of which is directed towards the windscreen through slots while others are used to control interior climate near the driver.

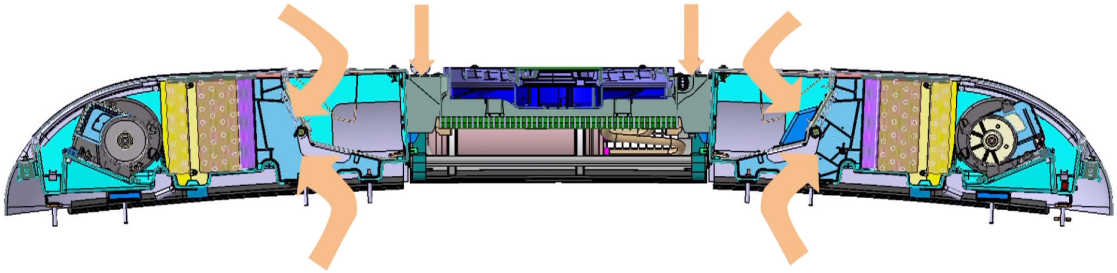

Figure 2.2: *Roof Top AC Unit*

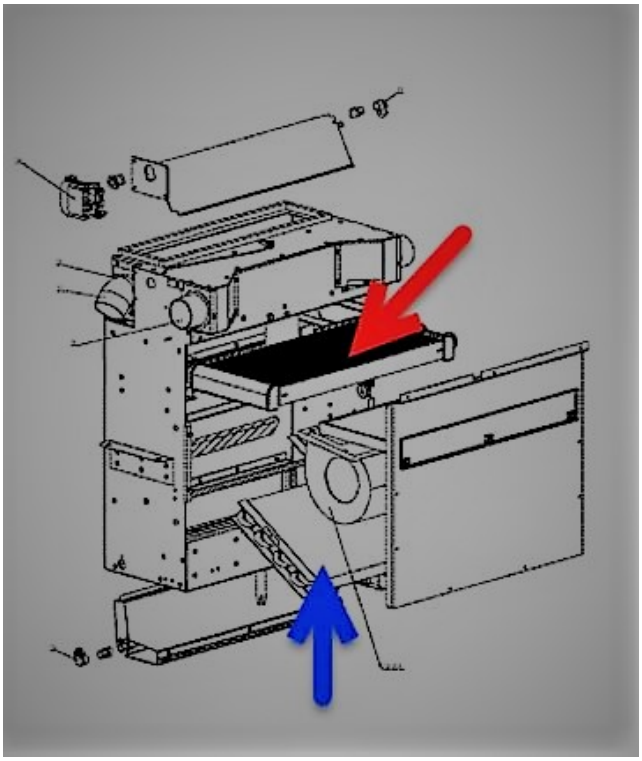

Figure 2.3: *Exploded view of a Defroster*

3

Method

In this chapter, the method followed to simulate the interior climate of the bus is presented. The choices made during the method development and reasons leading to those choices are discussed. The best practices described in the industry and by earlier studies are used as a first step to building the model. Method suggestions made on the online platform, Steve Portal[13], and the model descriptions made in the user manual[12] are used to guide the method development process.

The methodology is presented in two parts. The first part deals with the steady state modelling of the interior climate. In this, a model is built which represents a stable climate condition inside the bus. The second part discusses the changes made in the model to simulate the unsteady behavior of the interior climate. It also describes the methodology followed to simulate the door opening cycle.

3.1 Steady State Modelling

A steady state model solves the governing equation mentioned in chapter 2 without the derivative of time. Steady state simulation is an iterative approach which is used to find a stable solution i.e, solution which is not a function of time. Experiments were conducted to measure temperature at different points during a pull up or pull down cycle. In a pull-up cycle, the bus is soaked in a cold ambient temperature and then it is heated until the required temperature is attained. In a pull-down cycle, the bus is soaked in hot ambient temperature and is cooled until the required temperature is attained. The converged solution of the presented steady state model represents the end of the pull-up or pull-down cycle i.e, when the temperature inside the bus does no longer change with time.

3.1.1 Geometry

First step in the process of solving the problem was to prepare the geometrical representation or CAD(Computer aided Design) of the bus. This was done using pre-processing software called ANSA. The bus model was divided into three parts to make it easy for handling the CAD model in the software. It was divided based on the naming convention used in the industry which is shown in the figure 3.1. Parts of the divided model which required special mesh setting or required to specify boundary conditions were marked and given a name to identify them in StarCCM+. This is seen in the figure 3.2 where the seats, bars, windows and the body of the bus are represented by different colours. Parts of the bus which were not essential to model interior climate were marked separately and removed from the model in StarCCM+. Small holes and gaps in the geometry were closed in ANSA which would otherwise make it harder for meshing operation. Some surfaces were added to the model to simplify the geometry and to add the missing parts. Once the model was prepared in ANSA, it was transferred to StarCCM+ for the further process.

3.1.2 Mesh

To solve fluid flow the geometry is split into smaller domains which are made of simple geometric shapes. In these sub domains the governing equations are discretized and solved. Naturally, smaller size of these sub domains have better representation of the model but using smaller sizes would increase the number of these domains and computational resources required to solve. Hence, identifying the areas where fine mesh is required

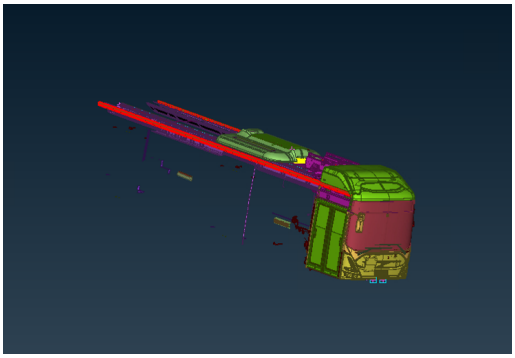

(a) *Front*

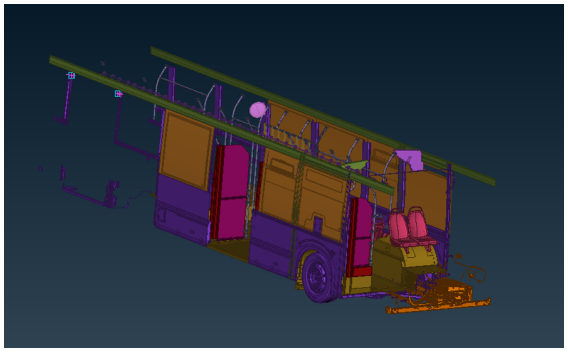

(b) *Middle*

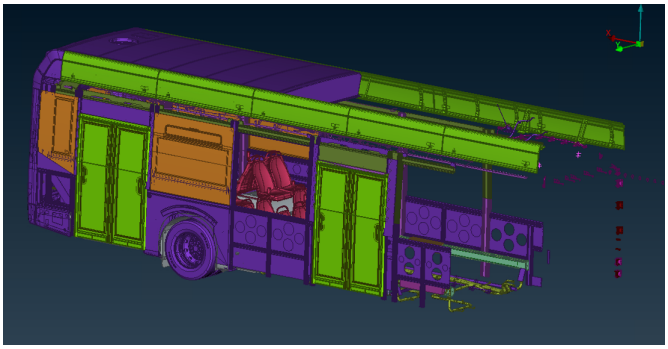

(c) *Rear*

Figure 3.1: *Division of model in ANSA*

becomes crucial. Therefore, meshing becomes an important step in the process of CFD as a good mesh strategy helps in finding accurate solutions.

3.1.2.1 Surface Wrapper

To obtain a good mesh a closed and non-intersecting geometry is necessary. Most of the geometry clean up is done in the pre processing step in ANSA. However an input from ANSA with no geometric faults such as gaps, intersecting or overlapping surfaces would be difficult to obtain and could take a lot of time. This is overcome using surface wrapper operation in StarCCM+. Surface wrapper can be pictured as sheet that is wrapped around a geometry which simplifies the geometry by covering all the small gaps and cleaning all the mismatches between the surfaces. A good surface wrap with surface remesher makes it easier to obtain a good volume mesh.

In the earlier study made on this bus[10], the surface wrapper operation is carried out in two steps. One wrapper with coarse settings to get a closed internal domain of the bus. Then a wrapper with fine settings with the details of the interior so that geometry in the volume of interest is not altered. To simplify the process this is replaced by a single surface wrapper with gap closure. In this method wrapper with fine settings is used and the volume of interest is specified by using series of seed points which are placed in areas where air would be present. This way the need for a separate coarse wrapper to define the volume of interest is removed.

The settings used in surface wrapper operation is summarised in the table 3.1.

In order to improve the quality of the mesh, surface remesher operation is carried out. Surface remesher retriangulates the surface to get a better starting surface for volume mesh. Figure 3.4 shows remeshed surface of the bus.

Figure 3.2: *Identification of different parts of the bus in ANSA*

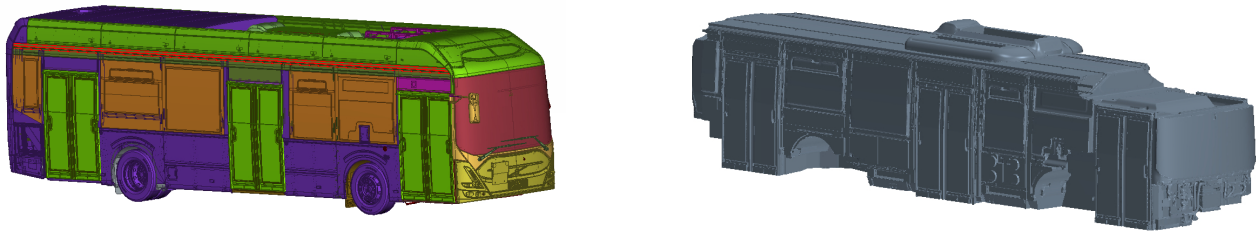

(a) *Actual Bus* (b) *Surface Wrapped part*

Figure 3.3: *Surface Wrapper*

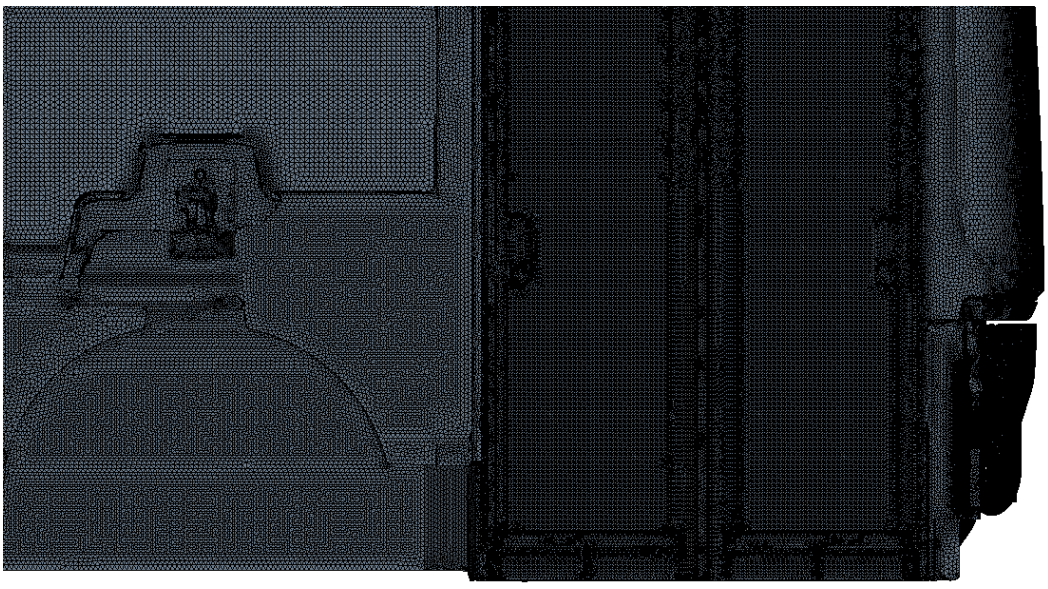

Figure 3.4: *Example of a remeshed surface*

Default Settings	
Base size	100 mm
Target surface size	30 mm
Minimum surface size	15 mm
Surface curvature	36.0
Gap Closure	Seed point
Volume of Interest	Seed points

Custom Controls		
Parts	Target Surface Size	Minimum Surface Size
Roof Unit	10 mm	5 mm
Air Duct	5 mm	2 mm
Bars, Handles & shields	10 mm	5 mm
Base Parts	15 mm	10 mm
Doors	10 mm	5 mm
Defroster	8 mm	5 mm
Mirrors	10 mm	5 mm
Heaters	5 mm	1 mm
Inlet Holes	1 mm	0.5 mm

Table 3.1: Surface Wrapper settings

3.1.2.2 Automated Volume Mesh

Volume mesh is generated in the domain using Automated mesh in StarCCM+. Polyhedral mesher along with prism layer mesher is chosen to mesh bus volume. Polyhedral mesher uses an arbitrary polyhedral shape in order to build the core mesh. Polyhedral mesher is used as it provides good quality results with lower cell count and also because of the pseudo-random orientation of the faces, polyhedral cells works better when the flow direction is different in different locations in the domain.[13]

The prism layer mesher is used to generate orthogonal cells next to the walls of the domain. These cells allow the solver to resolve the flow more accurately closer to the wall. Walls are generally a source of vorticity and therefore predicting flow around the walls becomes critical. The thin layer of the fluid close to the walls of the domain is referred to as boundary layer. This boundary layer is divided into three sub divisions: viscous sublayer, log layer and buffer region. Viscous sublayer is the layer closest to the wall and log layer is the layer in the farthest away in the boundary layer. Buffer region is the region in between viscous sublayer and log region. The extents of these layers are defined using a non dimensional number y^+ which is a function of absolute distance from wall and wall shear stress. $y^+ \sim 1$ signifies that the viscous sublayer is resolved and exact shear stresses are calculated. However this will increase the number of cells in the domain. An alternative solution to this is to have $y^+ \sim 30$, i.e. to place the first cell in the buffer region, and use wall functions to predict the shear stresses. Additionally, using all y^+ treatment in the turbulence model uses blended wall function that emulates the low y^+ treatment of fine meshes and high y^+ treatment of coarse meshes. This would mean that a y^+ value between 1 and 30 is preferred in the domain. Plot 3.5 shows a histogram plot of the wall y^+ distribution in the bus versus the frequency of occurrence. This shows that most of the cells in the domain have wall y^+ value of 10 or lower which signifies a good mesh around the walls.

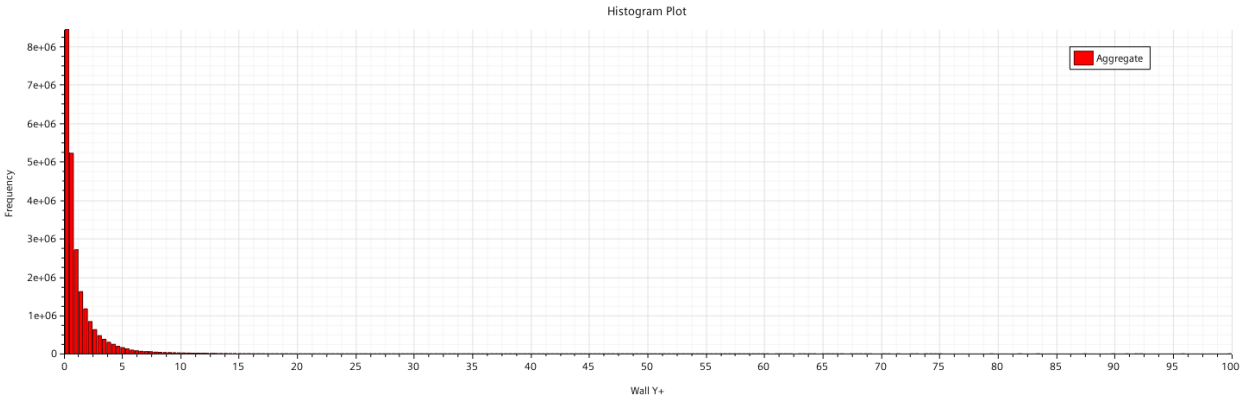

Figure 3.5: *Histogram of Wall y^+ in the bus domain*

All the heat exchangers, evaporators and porous media present in the domain are treated as separate regions

with interfaces between them and rest of the domain. These regions have to be meshed separately. Trimmed mesher is used to generate volume mesh in these regions. Trimmed mesher constructs a mesh using hexahedral cells that cuts or trims the core mesh using the starting surface mesh. In these regions flow is unidirectional and trimmed mesh with grid lines aligned to the flow gives better results.[13]

It is desirable to use a mesh which gives a stable solution with as fewer cells as possible. Many different mesh configurations have been tested to achieve this goal. Three of these configurations are presented here with the first mesh configuration having 150,000,000 cells, the second with 189,000,000 cells and the third with 230,000,000 cells. The figure 3.6 shows the steady state plots of temperature and velocity at different points inside the domain which are obtained from the first mesh configuration. Big fluctuations can be observed in the velocity plot at all points between iterations and big fluctuations can be observed in temperature plot at one of the points. This indicates an unstable solution.

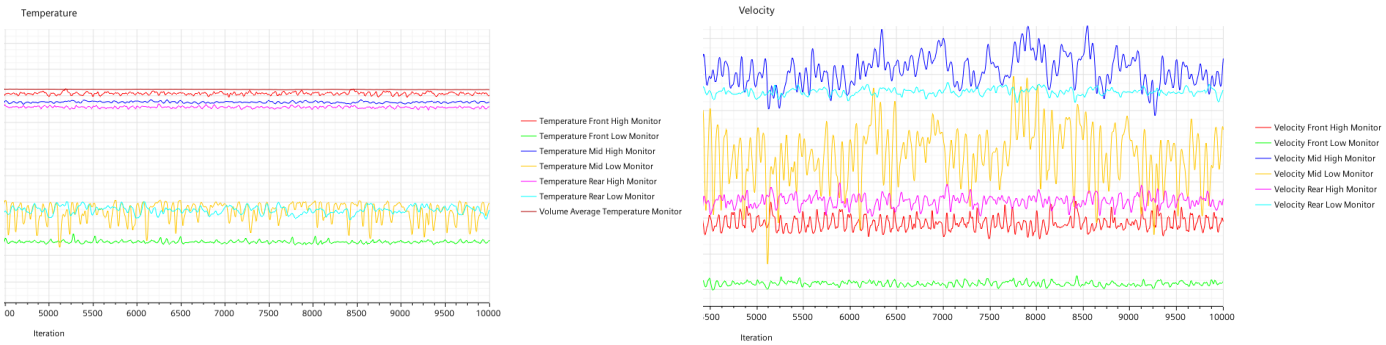

(a) *Temperature at different points inside the bus* (b) *Velocity at different points inside the bus*

Figure 3.6: *Results of the first Mesh configuration*

To overcome instability in the solution the mesh has been refined to get second mesh configuration. Figure 3.7 shows the temperature and velocity fluctuations resulting from this mesh. It can be observed that the fluctuations in the velocity and temperature plots have reduced in this mesh configuration when compared to the previous one. This mesh configuration is comparatively stable.

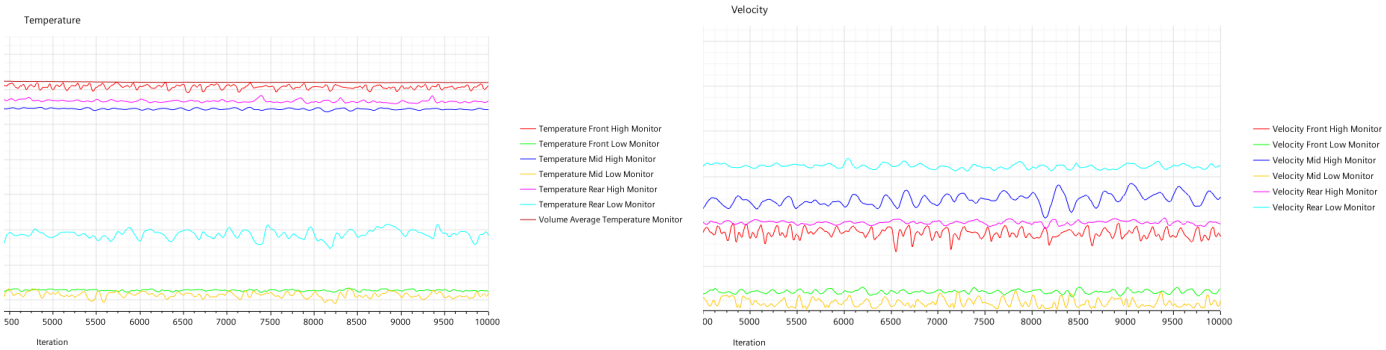

(a) *Temperature at different points inside the bus* (b) *Velocity at different points inside the bus*

Figure 3.7: *Results of the second Mesh configuration*

However, there are still some fluctuations in the solution between iterations in the second configuration. Figure 3.8 shows a very stable plots of temperature and velocity for the third mesh configuration which is further refined from the second configuration. Second and third configurations show similar plots except for the small fluctuations in the second configuration. Due to higher computational cost of the third mesh configuration it was decided to use second mesh configuration and average the field values of last 1000 iterations.

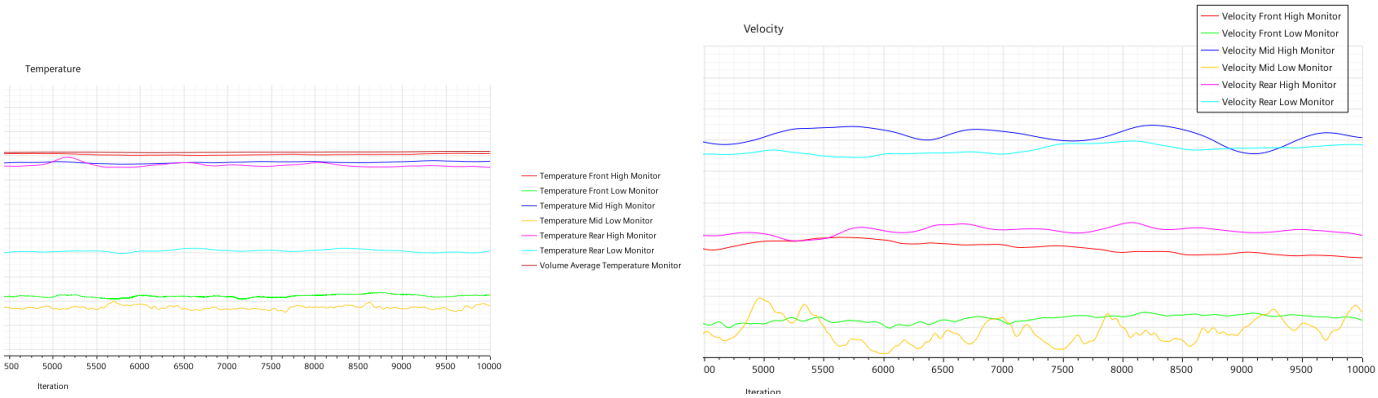

(a) *Temperature at different points inside the bus*

(b) *Velocity at different points inside the bus*

Figure 3.8: *Results of the third Mesh configuration*

3.1.3 Physics and Solver

In order to simulate fluid motion, it is necessary to choose models which collectively represent the problem at hand. This chapter details the models selected to simulate the interior climate of the bus. In this section reasons for selecting a model and changes made to default model settings are presented. The type of solver and solver settings used in the simulation is also discussed in this section.

3.1.3.1 Physics

Governing equations are solved in three dimensional space, in steady state and the properties of the fluid considered are that of air at atmospheric conditions. Gravity model is selected to obtain the effect on density with varying temperature. This defines the motion of the fluid due to natural convection.

Equation of state model are constitutive relations that describe the relation between density and the internal energy to the two thermodynamic variables, pressure and temperature. The two models for equation of state that are suggested by the StarCCM+ user guide[12] are constant density model and ideal gas model for natural convection problems. The ideal gas model solves the varying density when there are large vertical temperature gradient. In the previous study made on interior climate, it was found that buoyancy was better captured by using ideal gas model[10]. Therefore ideal gas model was selected as the equation of state.

Realizable k-ϵ turbulence model is selected to predict the turbulent scales in the simulation. This model is recommended and widely used in the industry. It is also possible to select two layer all $y+$ treatment with k-ϵ turbulence model. It is also recommended to change the two layer model from shear driven to buoyancy driven for flows where natural convection is dominant. Changing to buoyancy driven represented a more realistic case of natural convection. It can be observed in the middle of the figure 3.9 hot air which is lighter than cold air settles at the bottom of the bus with shear driven flow. This is not observed with buoyancy driven flow which indicates that buoyancy driven two layer model captures buoyancy effect better.

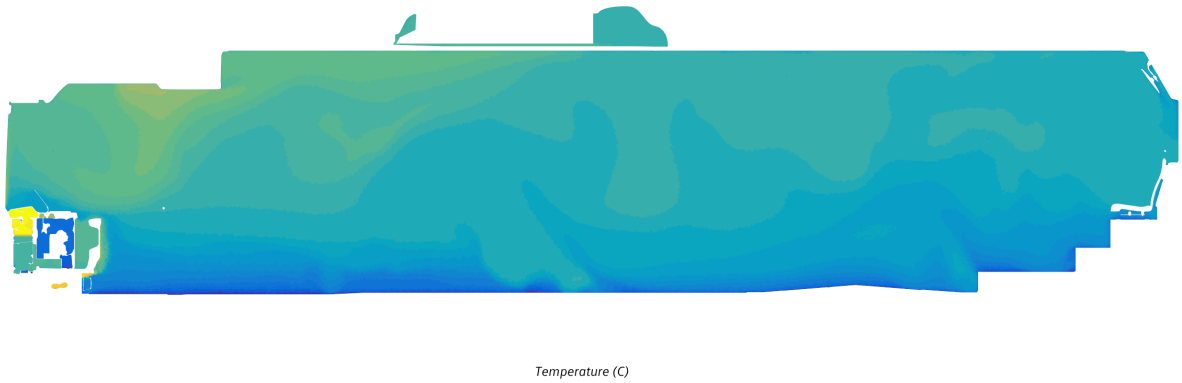

(a) *Shear driven flow*

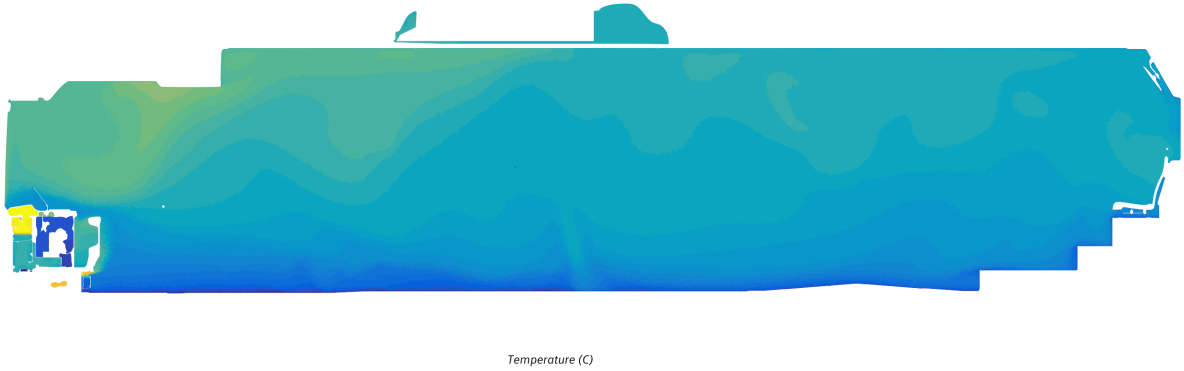

(b) *Buoyancy driven flow*

Figure 3.9: *Temperature distribution along the centre plane of the bus*

There are some models in StarCCM+ that are selected automatically and these can be considered as recommended settings. The list of chosen physics models are listed below in the table 3.2.

Model group	**Selected Model**
Space	*Three dimensional*
Material	*Gas*
Flow	*Coupled Flow* *Coupled Energy* (Automatically Selected) *Gradients* (Automatically Selected)
Equation of state	*Ideal Gas*
Time	*Steady*
Viscous Regime	*Turbulent* *Reynolds-Averaged Navier-Stokes* (Automatically Selected)
Turbulence Model	$k-\epsilon$ *Turbulence* *Realizable* $k-\epsilon$ *Two layer* *Two layer All y+ Wall treatment* *Wall*(Automatically Selected)
Optional Model	*Gravity* *Cell Quality Remediation*

Table 3.2: List of selected Physics Models

3.1.3.2 Solver

The Coupled Flow model solves the conservation equations for mass, momentum, and energy simultaneously using a time-marching approach. In a steady state simulation, a pseudo-transient term replaces the physical time derivative. The solution in each cell is advanced independently with an optimal pseudo-time step computed locally according to a Courant-Friedrichs-Levy(CFL) number specified. It is also possible to select an automatic method to choose the CFL number. In this method, a CFL number as high as possible that satisfies the convergence criterion of the solver is used. The advantage with coupled solver is that the solution can be accelerated by using high CFL number to obtain convergence in fewer iteration. Another advantage of the coupled solver is that the rate of convergence does not deteriorate with mesh refinement.[13] One of the disadvantages with the coupled solver is the memory requirements which was not an issue because of the available resources in the industry.

3.1.4 Boundary Conditions

The boundary condition is a condition in which a value varying in the rest of the domain must satisfy at the specified boundary. Boundary conditions are necessary constraints to solve a boundary value problem. These constraints can also be used to construct model as close to reality as possible. This section describes how boundary conditions at each of the components of HVAC discussed in chapter 2 are defined to simulate interior climate.

In the earlier study made on interior climate[10], an open system is modelled to simulate interior climate. In that study, inlets and outlets are used at the entry and exit regions of the roof unit and defroster. Thus eliminating the need for modelling the air inside roof unit and the defroster. However, in reality the air entering roof unit and defroster is recirculated back into the cabin. There are no outlets in the domain except for some leakage losses. These losses are unknown and hard to model. So ignoring the losses, in this thesis the interior climate is modelled in a way where there is complete re-circulation of air. There are no inlets or outlets in the model, air is allowed to move freely inside the roof unit and defroster. The heated or cooled air is then pushed back in the cabin by using fans.

3.1.4.1 Roof Top Air Conditioning Unit

The roof top unit is modelled to work in a similar way that is explained in the chapter 2. Air enters from cabin to the roof unit either on the right or left side through the ducts as shown in the figure 3.10. Air is then passed through an evaporator before it is blown in to the ducts. Evaporator is modelled as a single stream heat exchanger in which heat from hot air is removed in cooling mode. In heating mode, this evaporator is considered as a heat exchanger and heat is added to cold air. This simplification removes the need for separate modelling of heat blower.

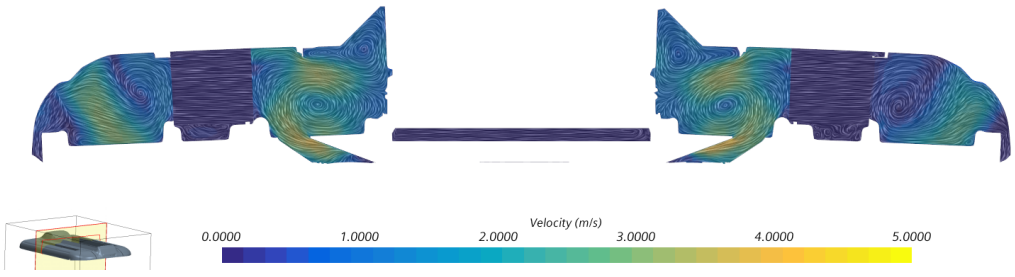

Figure 3.10: *Velocity Vector at a plane along the length of the bus*

Evaporator consists of tubes through which coolant passes and fins which increase the heat transfer rate from air to the coolant. Air passing through the small gaps between the fins of the evaporator results in a pressure drop. Evaporator is modelled as a porous region to model the pressure drop of air passing it. Porous region is

a region that is permeated by number of pores.

Equation 3.1 is an empirical model for pressure drop δP over a length L based on Darcy's law that describes fluid flow through porous medium.[13]

$$\frac{\delta P}{L} = -(P_i|v| + P_v)v \tag{3.1}$$

P_i is the inertial resistance, P_v is the viscous resistance and v is the velocity. These coefficients have to be estimated to model the pressure drop. Experimentally found pressure drop over a range of flows for the particular porous medium is used to estimate these coefficients. The experimental data is plotted and a quadratic curve is fitted. The linear and quadratic coefficients of fitted curves gives the viscous and inertial porous resistance respectively. Figure 3.11 shows an example of fitting a quadratic curve to the experimental values of pressure drop.

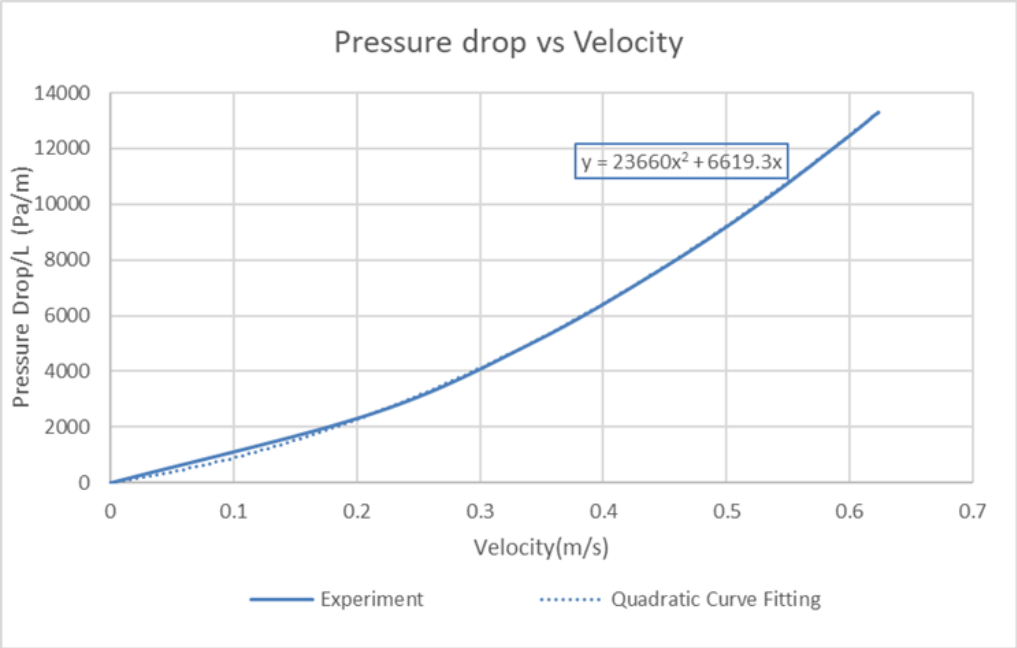

Figure 3.11: *An example of curve fitting the experimental pressure drop to get porous coefficients*

However, the experimental data for evaporator pressure drop in the roof unit was not available. To overcome this, the experimental data available for the evaporator used in defroster is scaled with the dimensions of the evaporator of the roof unit. The coefficients were then used in a free stream simulation to measure the volume flow output from the roof unit. This value was within 3 percent of the experimentally measured maximum volume flow rate of the roof unit. Figure 3.12 shows pressure distribution on a plane cutting through the roof unit. Drop in air pressure along the width of the evaporator can be observed in the picture 3.12.

These heat exchangers are single stream heat exchangers i.e, a black box which absorb or release heat so the subsequent heat transfer to the coolant is not modelled. Hence the condenser unit, where coolant is cooled, is removed from the simulation. This is the empty space that is seen in center of the picture 3.10 and 3.12.

The air passing through the evaporator is pushed into the ducts by 3 blower fans on each side of the roof unit. A very fine mesh would be needed if an actual blower is used in the model and it would be computationally expensive. As an alternative, blower fan performance curve can be used to model the fan. Blower fans are simplified as a rectangular blocks. They are considered as different region with an inlet and an outlet interface with the rest of the bus volume. The fan curve obtained from the manufacturer shown in figure 3.13 is used at the inlet interface of the region. The three curves shown in the plot correspond to three different speeds. The rectangular now block behaves like a fan by giving volume flow corresponding to the pressure at inlet interface.

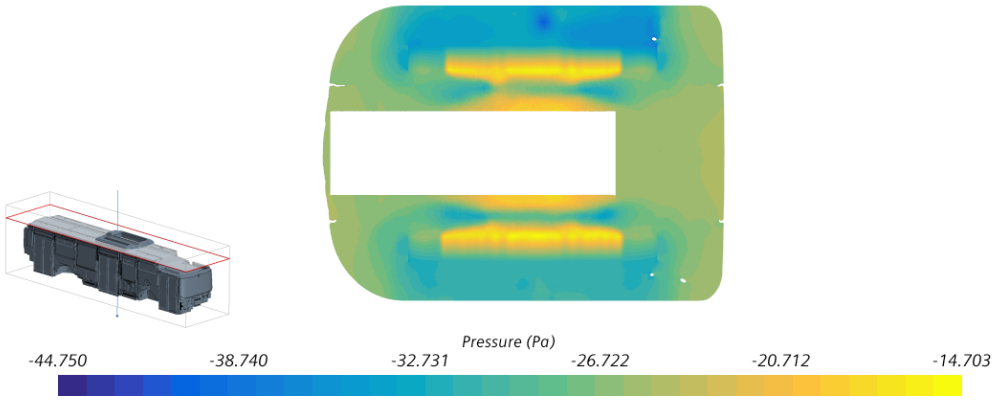

Figure 3.12: *Pressure distribution along a plane*

This also highlights the importance of correctly modelling the pressure drop across the evaporator to get the correct volume flow out from the roof unit. The working of blowers fans of pushing air into the duct can be observed in the velocity vector plot, see figure 3.14.

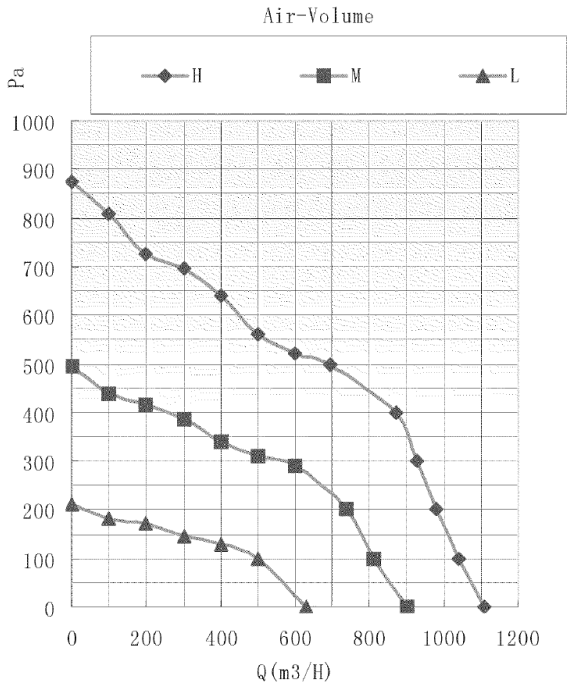

Figure 3.13: *AC Blower Fan Performance Curve*

3.1.4.2 Defroster

The air is allowed to enter naturally into the defroster at the front of the bus. Air passes through a evaporator before it is pushed upwards by a blower fan. The air forced out of the blower passes through an air filter and a heat exchanger before reaching the cabin. All the components of the defroster are also modelled in a similar way to that of roof top air conditioning unit. Evaporator, air filter and heat exchanger are all modelled as porous media to get the drop in pressure of air across them. Figure 3.15 shows plots of pressure drop versus velocity for evaporator, air filter and heat exchanger respectively and the corresponding quadratic curve fitting

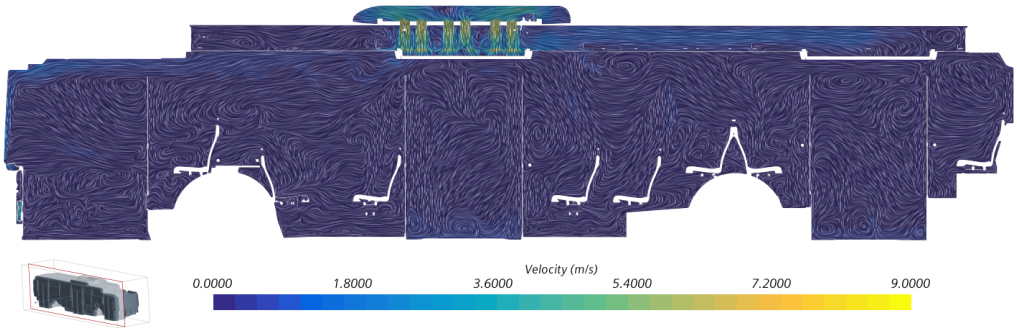

Figure 3.14: *Velocity along a plane*

coefficients. These coefficients are used to describe the porous medium in StarCCM+.

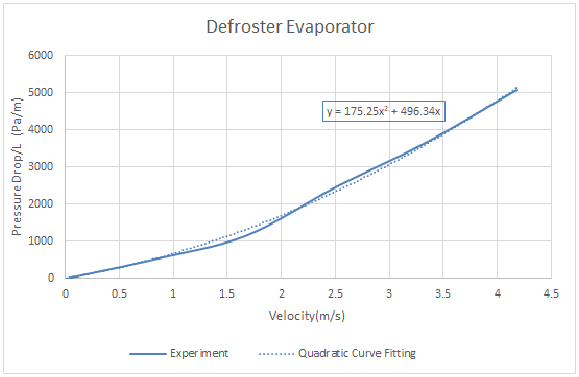

(a) *Evaporator*

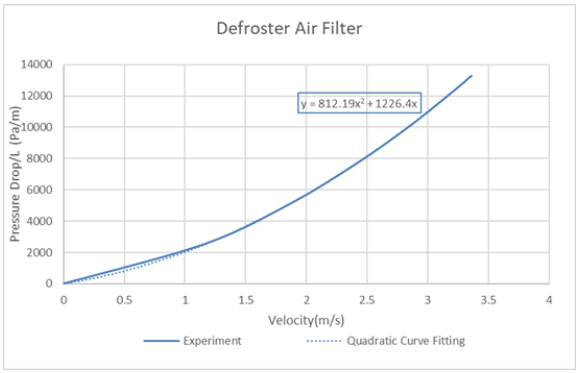

(b) *Air Filter*

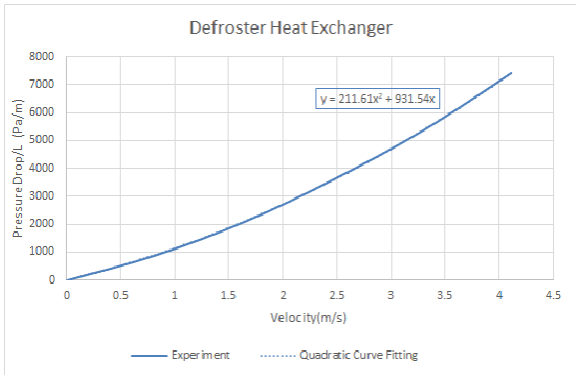

(c) *Heat Exchanger*

Figure 3.15: *Pressure drop versus velocity for different components of defroster*

During the heating mode, heat is added to air at the heat exchanger and during the cooling mode heat is extracted at the evaporator. Therefore, the energy source option is switched to heat exchanger for the defroster heat exchanger during the heating mode and for the evaporator during the cooling mode. The amount of heat removed or added is computed by solver with the specified exit temperature of air which is obtained through experiments.

The blower fan present in the defroster is modelled exactly like the fans in the roof unit. The fan curve obtained from the manufacturer is fed to the fan interface to get the corresponding volume flow out. Figure 3.16 shows the velocity distribution and pressure contour on a plane cutting the defroster. Pressure drop across evaporator at the bottom and across air filter-heat exchanger at the middle is clearly visible. The high velocity out from two outlets of the blower fan before the air filter region can also be observed in the figure 3.16.

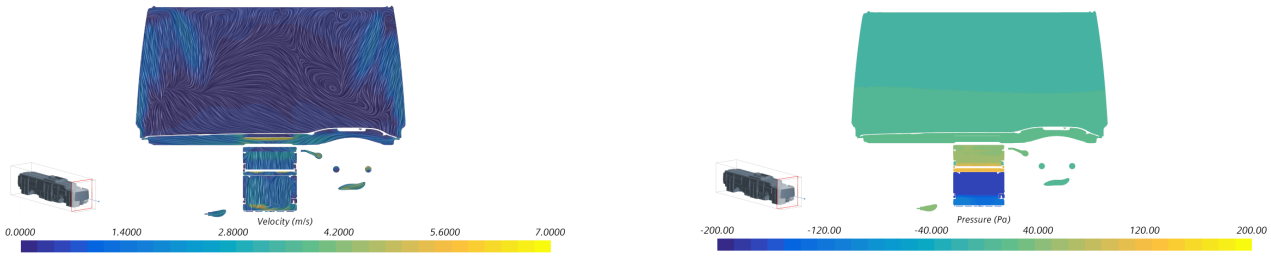

Figure 3.16: *velocity distribution(left) and pressure contour(right) on a plane cutting the defroster*

3.1.4.3 Convectors and Heaters

Convectors and heaters are modelled as a block where the heat is transferred to the air passing through them. These are treated as separate regions in StarCCM+ which means that they have to be wrapped and meshed separately. An inlet and outlet interface is created at the bottom and top of the block respectively. The energy source option for this region is selected as heat exchanger. The amount of heat rate at each of these convectors and heaters is different. It is calculated by multiplying heat rate per meter with the length of the heat exchanger. So, longer convectors give out more heat to air than shorter convectors. Heat rate per meter depends on the temperature difference between hot water and surrounding air. It also depends on the mass flow rate of the water in the convector.

The only difference between convector and heater is that heaters are equipped with fans to spread the heat released. This can be modelled by changing the momentum source option to ”specified” and adding the fan curve provided by manufacturer. Fans are only switched on when the doors are open and the temperature inside the bus is below set temperature. In other scenarios heaters are similar to the convectors.

3.1.4.4 Convection

A large amount of heat is transferred between the interior of the bus and the surrounding atmosphere. This heat is transferred through roof, floor, windows, walls and the doors of the bus. The heat transfer through a wall as shown in figure 3.17 is given by equation 3.2.

$$Q = U * A * (T_1 - T_2) \tag{3.2}$$

where Q_x is the amount of heat transfer through the wall, U is the overall heat transfer coefficient, A is the cross-sectional area, T_1 is the interior temperature and T_2 is the ambient temperature. The heat transfer coefficient is the combination of convective and conductive heat transfer which is given by equation 3.3.

$$\frac{1}{U} = \frac{1}{h_1} + \frac{L}{k} + \frac{1}{h_2} \tag{3.3}$$

where h_1 is the convective heat transfer coefficient between interior region and the inner surface of the wall, L is the length of the wall, k is the conductive heat transfer coefficient and h_2 is the convective heat transfer coefficient between exterior region and the outer surface of the wall.

This boundary condition can be set at the walls that are in contact with ambient air by changing the thermal specification to convection. All the parts interior to these walls have adiabatic thermal specification. When thermal specification is changed to convection, ambient temperature and heat transfer coefficient(HTC) have to be specified. The convective heat transfer between the wall and the interior region , h_1 in the above example, is calculated by the solver itself. For this interior wall temperature, T_w1 in the above example, would

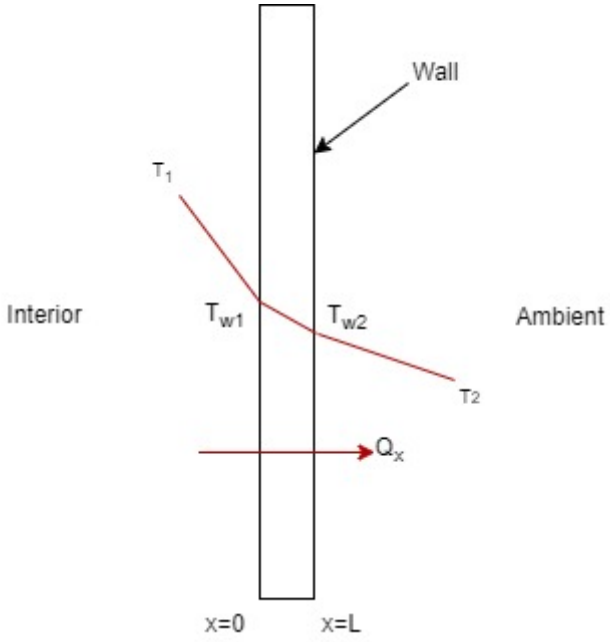

Figure 3.17: *Heat transfer through a wall*

be needed and is calculated with the help of HTC specified by user at the boundary. The conductive heat transfer through the thickness of the wall is different parts as conductive heat transfer coefficient depends on the type of the material and thickness of the material. In an another study, the conductive heat transfer coefficients of floor, roof, windows, wind shield and doors for this bus are calculated by using an average thickness for each of these parts[14]. These values are used as an initial estimate for HTC. The convective heat transfer between external wall and the ambient air is unknown. To overcome this, a scaling factor is multiplied with this initial estimate and swept over a range of values until the temperature inside the bus matched with the experimental data.

3.1.5 Experimental Data

The experiment was conducted in a climate chamber where the ambient temperature is controlled to represent three cases. A very cold case with -8.3 °C, a cold case with -4.5 °C and a warm case with 32 °C. The data used in the steady state simulation is extracted from either pull-up or pull-down tests. In these tests, the bus is soaked with one of the ambient temperature cases considered until all the measurement points have ambient temperature. Then the HVAC system is turned on and the bus is heated or cooled to get a particular set temperature. Set temperature is measured by taking weighted average between a point below the seat in the back left and a point at the top near the recirculating air intake of the roof unit. The set temperature is calculated to reflect an average temperature in the bus. HVAC control system uses set temperature to check if the required temperature is attained inside the bus. When the sensors measuring temperature inside the bus have stabilized, it is assumed to have attained steady state. The doors are completely closed during these tests and there is complete re-circulation of air inside the bus.

Apart from the points from where set temperature is measured, temperature is measured at six different points inside the bus. These points are placed in two different heights along the middle passage of the bus, see figure 3.18.

3.1.6 Calibration

As mentioned in the section 3.1.4.4, a part of the convection is unknown and a scaling factor is swept through a range of values to match the experimental data. Initially, the values from the study made U value estimation study[14] is used as HTC at the walls of the bus. These values are then multiplied with a scaling factor which represents the unknown convection part at the boundary, the unknown leakage losses and other

Figure 3.18: *Position of temperate measurement points.*

unknown errors in the model. The scaling factor is then changed to match the experimentally measured temperature at the six points. This way a correct value for HTC could be found and the errors in the model can be minimised. A larger HTC value in a cold case would let more heat out of the bus and in a warm case more heat is added to the bus from environment. Hence, this is case dependent and a calibration has to be carried out for each of the weather conditions. The weather condition considered in this thesis is -8.3°C.

3.2 Unsteady Model

In this section the changes made to the calibrated model to convert it into an unsteady model are presented. This unsteady model is used to simulate the door opening cycle. Door opening cycle is a standard cycle with 20s of door opening followed by 2 min of closed doors. The aim of this model is to evaluate the effect of the door opening cycle on the interior climate.

3.2.1 Geometry

A block around the bus is created in ANSA to represent the climate chamber. This is done to simulate the cold or hot ambient air interacting with the bus cabin when the doors are open. Figure 3.19a shows the climate chamber block which is 32.31m long, 7.08m wide and 5.63m high in x,y and z directions respectively. This resembles the climate chamber that is used for experiments.

In the calibrated model, the convection is modelled with no air flow on the exterior part of the bus. To use the same convection modelling another block is created closer to the bus surface. This block separates a region between the exterior of the bus and climate chamber which is not meshed. Therefore, there is no air flow around bus exterior and the calibrated model is still valid. The inner block is connected to the bus around the circumference of the doors as shown in figure 3.19b. This forms a small passage when the doors are open which makes it possible to simulate the interaction between air inside the cabin and the ambient air.

The front, middle and the rear doors are marked and named into two parts each as shown by different colours in figure 3.19b. This is done so that motion can be set to each half of the door to open and close them.

3.2.2 Mesh

The changes have been made to mesh to incorporate the new blocks and to facilitate the motion of the doors. The motion of the doors is obtained by using mesh strategy called overset mesh. This is also known as Chimera method in which one or more moving meshes are patched to a stationary background mesh. The moving mesh and the stationary mesh exchange flow field information at the interface between the two meshes. This interface is created in a two step process. In the first step, active, inactive and acceptor cells are determined. Cells that are at the boundary of each mesh(moving or stationary) are considered as the active cells. A cell is created

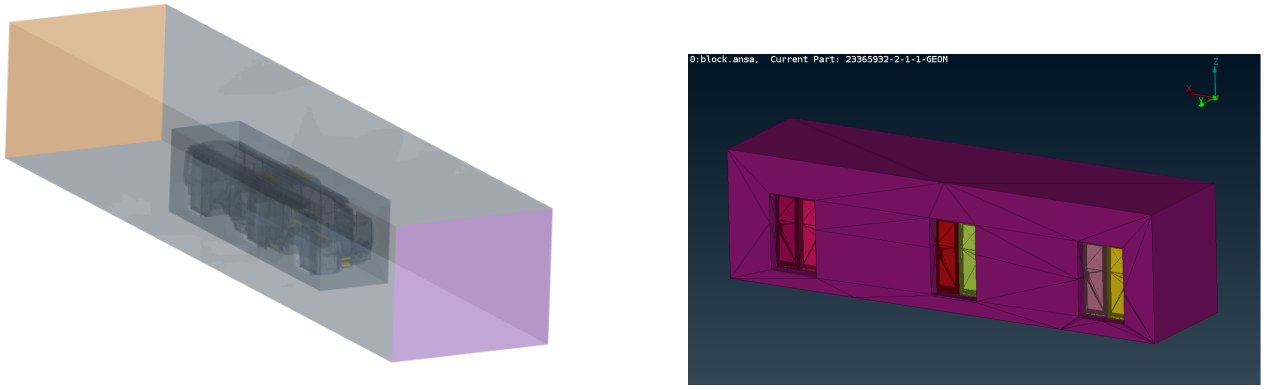

(a) *Representation of Climate Chamber* (b) *Inner block to separate a volume around the bus*

Figure 3.19: *Geometry changes for the Unsteady model*

next to these active cell which are known as acceptor cells. The second step is to ensure that there are donor cells surrounding each acceptor cell. Donor cells are used to determine the contribution of the exchanging flow-field information at the interface.[13]

To move the doors using overset mesh methodology, a background mesh and a separate mesh for the doors overlapping the background mesh is required. For this purpose, the new blocks created are included and the doors are excluded from the surface wrapper which forms the background mesh.
Each half of the door is meshed separately and is enclosed in a volume. The door and the enclosing volume together form a separate region known as overset mesh region, see figure 3.20. The volume enclosing the door is set as the overset boundary. This mesh overlaps the existing background mesh. In the next step, an interface between the background region and overset mesh region is created which is known as zero gap overset interface. Zero gap interface is used when there is no gap between the parts inside the overset mesh and the background mesh. Another zero gap overset interface is created between the two overset regions comprising of the door halves which overlap each other. In total 9 interfaces are created for 3 doors. When these interfaces are initialized, a hole cutting algorithm cuts a hole through the mesh in the shape of the door and stitches a single volume mesh, see figure 3.21.

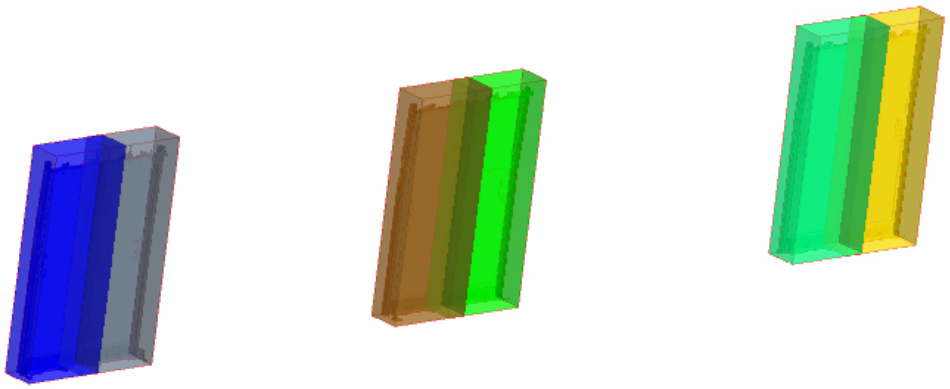

Figure 3.20: *Representation of overset volumes enclosing each half of the door*

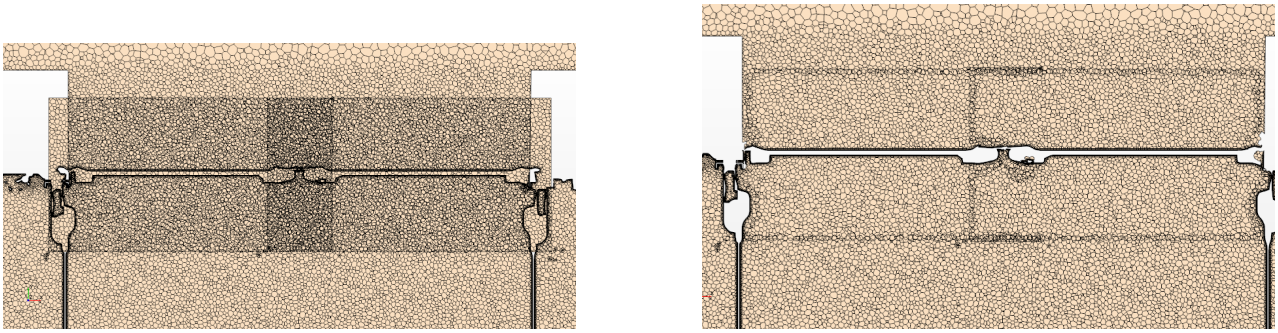

(a) *Before* (b) *After*

Figure 3.21: *Volume mesh representation before and after initializing the interfaces*

It is important to have a similar mesh size across the interface of both regions.[13] For this reason polyhedral mesh with the same size as that of the interior of the bus is chosen for the overset region. Large polyhedral cells are used to mesh the climate chamber because of its simple geometry, see figure 3.22. This makes sure too many cells are not introduced and the simulation is not very expensive in terms of computational power.

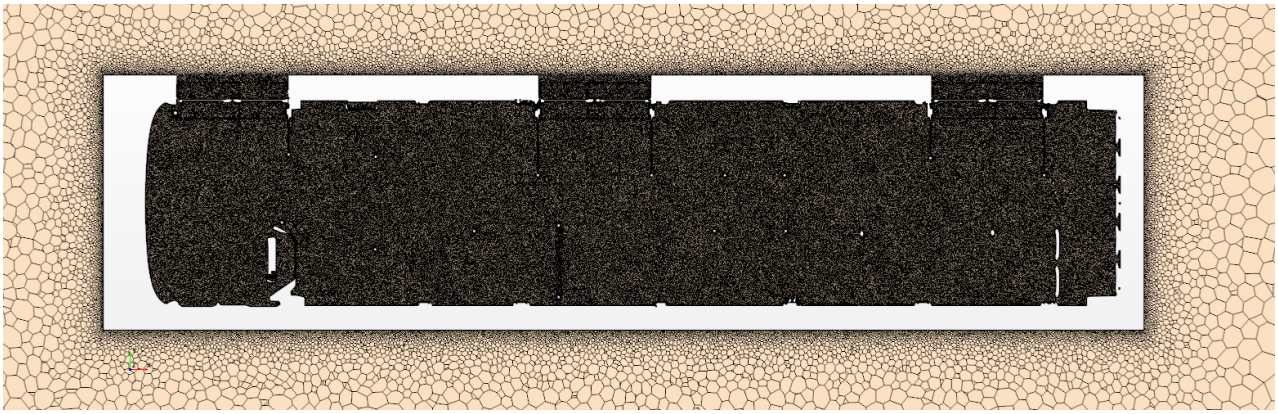

Figure 3.22: *Final representation of volume mesh along a plane for the entire domain*

3.2.3 Physics and Solver

All the physics models that are selected for the steady state are used in the unsteady model as well. The only change is made by switching time domain from steady to implicit unsteady. In implicit unsteady method, solution is calculated by both the current state of the system and the future state of the system. Since the future state of the system is unknown this is done iteratively. The time step choice for this model is derived from the requirement of the overset mesh methodology. It is necessary for the overset mesh, when in motion, to not move more than one neighbouring cell layer in a given time step.[13] Another requirement was that the door should close or open completely in 2 seconds from the start of its motion. Using these two requirements, a maximum time step that could be used was found to be 0.02s. Since the simulation had to run for 2 min to complete the door opening cycle and is very expensive in terms of computational power to run this long, it was decided to use the maximum possible time step. Initially the simulation is run without any door motion and with 5 inner iterations, the magnitude of the residuals seem to drop at each time step which can be seen in the figure 3.23.

3.2.4 Boundary Conditions

All the boundary conditions that have been modelled in steady state are left intact except for the heaters. When the doors open, the temperatures inside the bus for the considered case will drop and heaters needed to be turned on to spread the heat. A fan curve is fed to the heaters and a constant heat output is set to all the

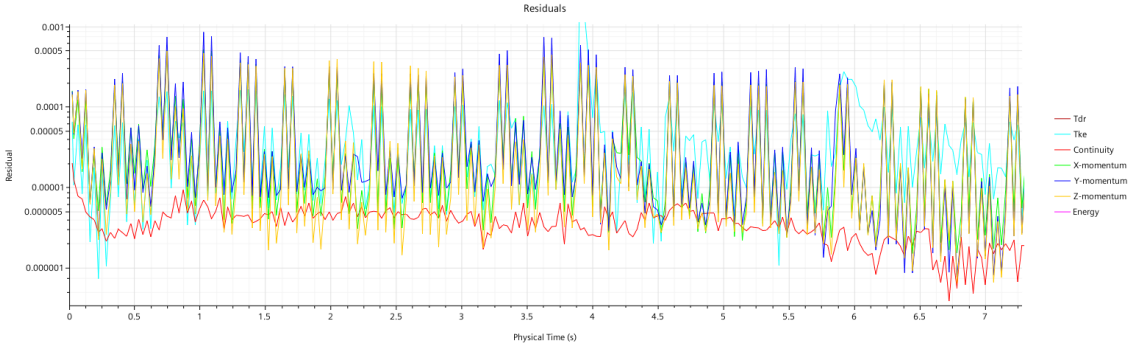

Figure 3.23: *Plot of residuals versus time for the unsteady model*

heaters that is given by the manufacturer. Figure 3.24 shows the temperature distribution plot which shows the working of the heaters at time instant while the doors are opening. The inlet of the climate chamber is set to stagnation inlet condition with atmospheric pressure and temperature of -8.3°C. The outlet is set to pressure outlet condition with atmospheric pressure and temperature of -8.3°C. The rest of the walls are set to symmetry plane with temperature of -8.3 °C.

Figure 3.24: *Temperature distribution plot at a time instant showing the working of heaters*

Motion of the door is obtained by changing the motion specification from stationary to rotation for the overset region. Rotation of the doors is controlled by a time dependent field function. The field function output is shown in the plot made between door rotation and solution time, see figure 3.25. When the solution time is between 4 and 5.8 seconds, each half of the door is rotated one degree every time step. Between the solution time of 5.8 and 26 seconds the door rotation value is set to 90 degrees to keep the doors open for 20 seconds. Then the rotation value is reduced by 1 degree at each time step during the solution time from 26 to 27.8 seconds.

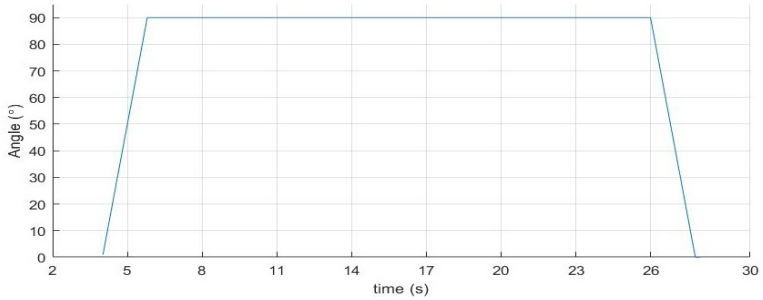

Figure 3.25: *Motion of door versus physical time*

4

Results

In this chapter, the results from a simplified model are presented which shows a proof of concept for the type of modelling described in section 2.4. This is followed by the steady state model calibration results and the door opening cycle results.

4.1 Simplified Model

To understand the challenges of modelling with complete recirculation and no outlets a simplified model is built. Figure4.1 shows a simplified bus geometry with rectangular boxes representing roof air conditioning unit and defroster unit. All the other HVAC components are also simplified and modelled in the way described in the section 2.4. The results from the simplified bus model are shown in figure 4.2. It can be observed that the residuals drop 3 orders of their initial value and the temperature at six different points inside the bus are reasonably stable at the end of simulation. It can also be observed that all the lower points have lower temperature when compared to the higher points which showing correct modelling of natural convection. This is considered as proof of concept and similar modelling is implemented in the actual bus.

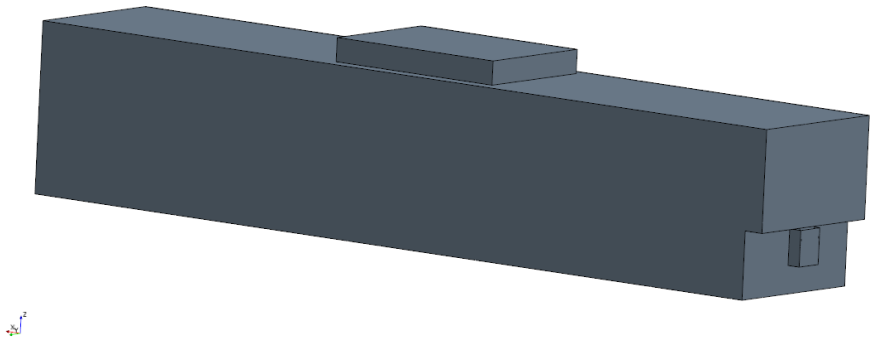

Figure 4.1: *Simplified bus geometry*

4.2 Steady State Model

In this section, the results from the steady state model are presented. Initially the results from the calibration sweep to find the HTC are presented and discussed. This is followed by the discussion on criterion that is used to judge convergence of results and converged plots of temperature are shown. Then the three dimensional flow fields are presented which shows the model capturing the expected and realistic flow around the bus. These are followed by three dimensional picture of the temperature distribution in the bus. The following sub section shows how heat is lost from the interior of the bus through the walls and discuss which parts of the bus exterior have higher convective heat transfer.

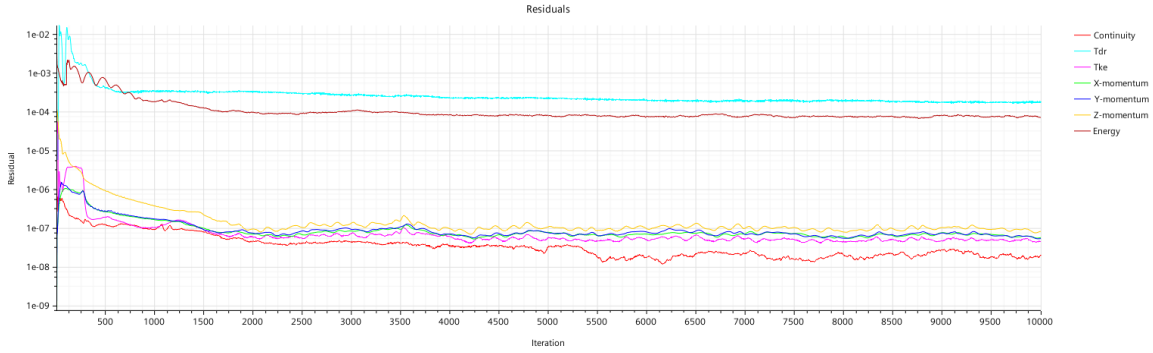

(a) *Residuals*

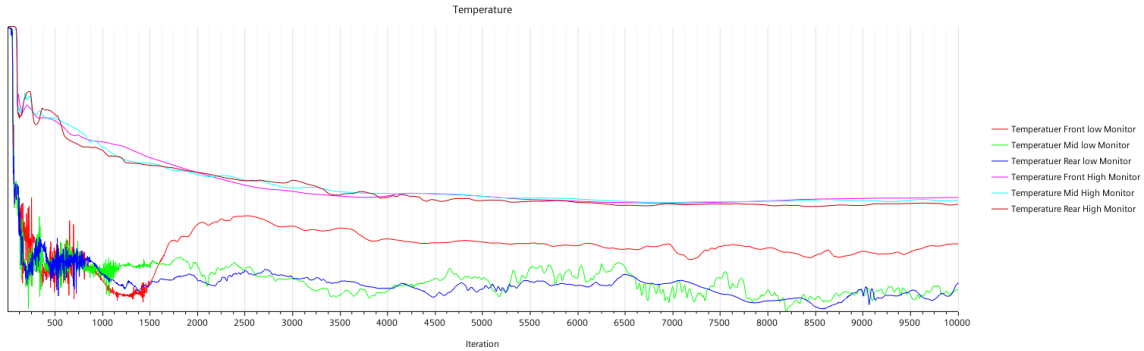

(b) *Temperature of six different points inside the bus*

Figure 4.2: *Results from a simplified bus*

4.2.1 Calibration sweep

A scaling factor was multiplied with the initial heat transfer coefficient(HTC) values obtained from the study made on U value estimation[14]. This scaling factor represents the unknown part of the heat transfer coefficient at the walls. Scaling factor varies in the range of 0.1 to 1. Simulation is run until convergence is achieved for each of this scaling factor value. Then, plots are made between the difference in temperature at the measured points from simulation and experiment versus the scaling factor. These plots are presented in this sub section. A horizontal line in the plots at zero temperature difference represents the experimental temperature. Points along the curve represent how far they are away from experimental data. A negative value represents the temperature from simulation which is colder than experiment and a positive value represents the temperature from simulation which is warmer than experiment.

Figures 4.3-4.5 are the plots showing variation of difference in temperature versus scaling factor. A plot has been made for each individual measuring point from the experiments. The ambient temperature considered for this case is -8.3°C.

From all the plots, we can see that a larger scaling factor which represents large HTC lowers the temperature inside the bus. As the scaling factor is decreased, the bus gets warmer. This is because with large HTC there is more convective heat transfer between the interior and the ambient air and heat from inside the cabin is lost to the surroundings.

The shape of the curves for all the plots are similar. In general the lower points needed a smaller scaling factor when compared to higher measuring points. This is because in study made on U value estimation [14] a larger value of HTC was estimated at the floor when compared to other parts of the bus. Hence, it had to be scaled down by larger factor when compared to the higher points. However, the rear low point did not need a large factor to increase the temperature from initial value which was hotter than the other lower points. This is because of the effect of hot air leaking from the roof unit on to the floor which is shown in the section 4.2.3.

We can also observe that at each of the measuring points, a different scaling factor is needed to match

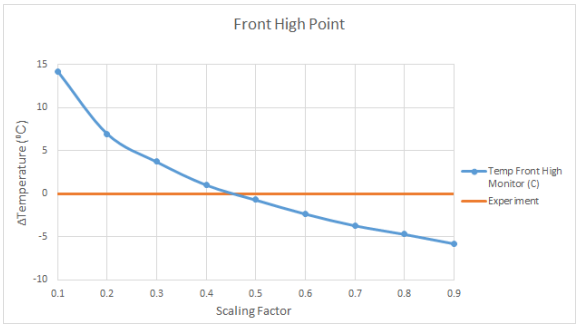

(a) *Front high*

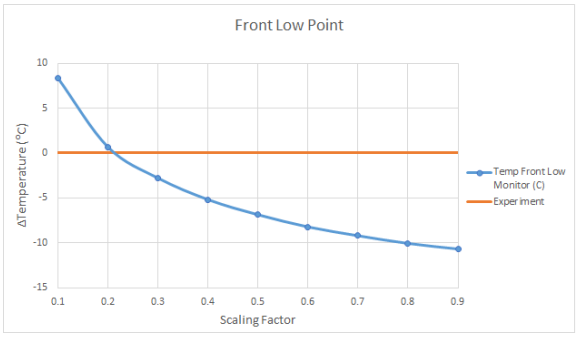

(b) *Front low*

Figure 4.3: *Scaling factor versus temperature difference between experiment and simulation for the points in front*

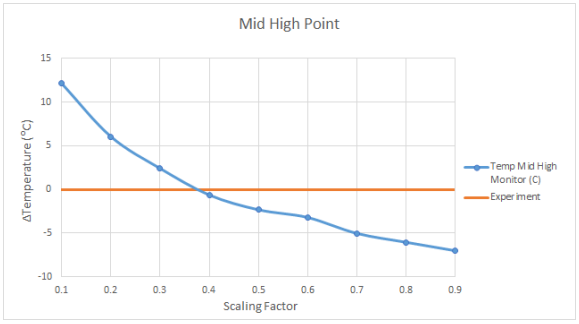

(a) *Middle high*

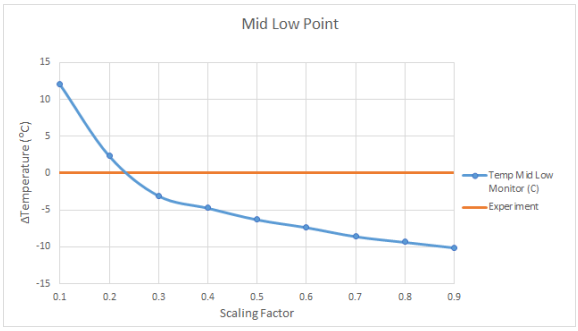

(b) *Middle low*

Figure 4.4: *Scaling factor versus temperature difference between experiment and simulation for the points in middle*

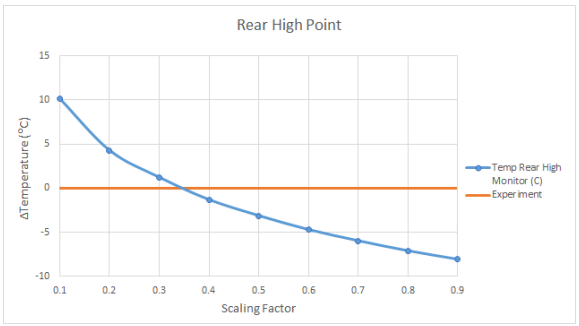

(a) *Rear high*

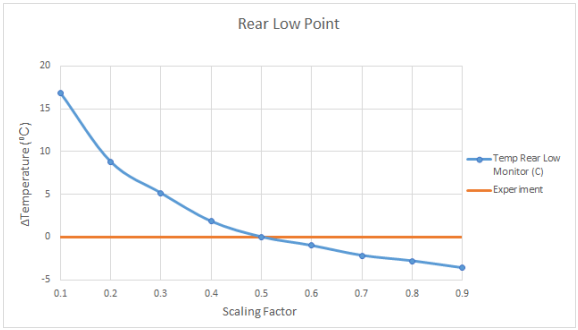

(b) *Rear low*

Figure 4.5: *Scaling factor versus temperature difference between experiment and simulation for the points in the rear*

temperature to the experimental value. However, a single scaling factor is required to find the unknown part of the HTC. To overcome this problem, the temperature at all the six points is averaged in both experiment and simulation and then the difference between these averaged values is plotted versus scaling factor, see figure 4.6. In this plot we see a trend line that is similar to the individual points trend line. The six point averaged temperature in the simulation matches the experimental value when a scaling factor of 0.33 was multiplied with the initial HTC values. This is used in the final simulation for the steady state model.

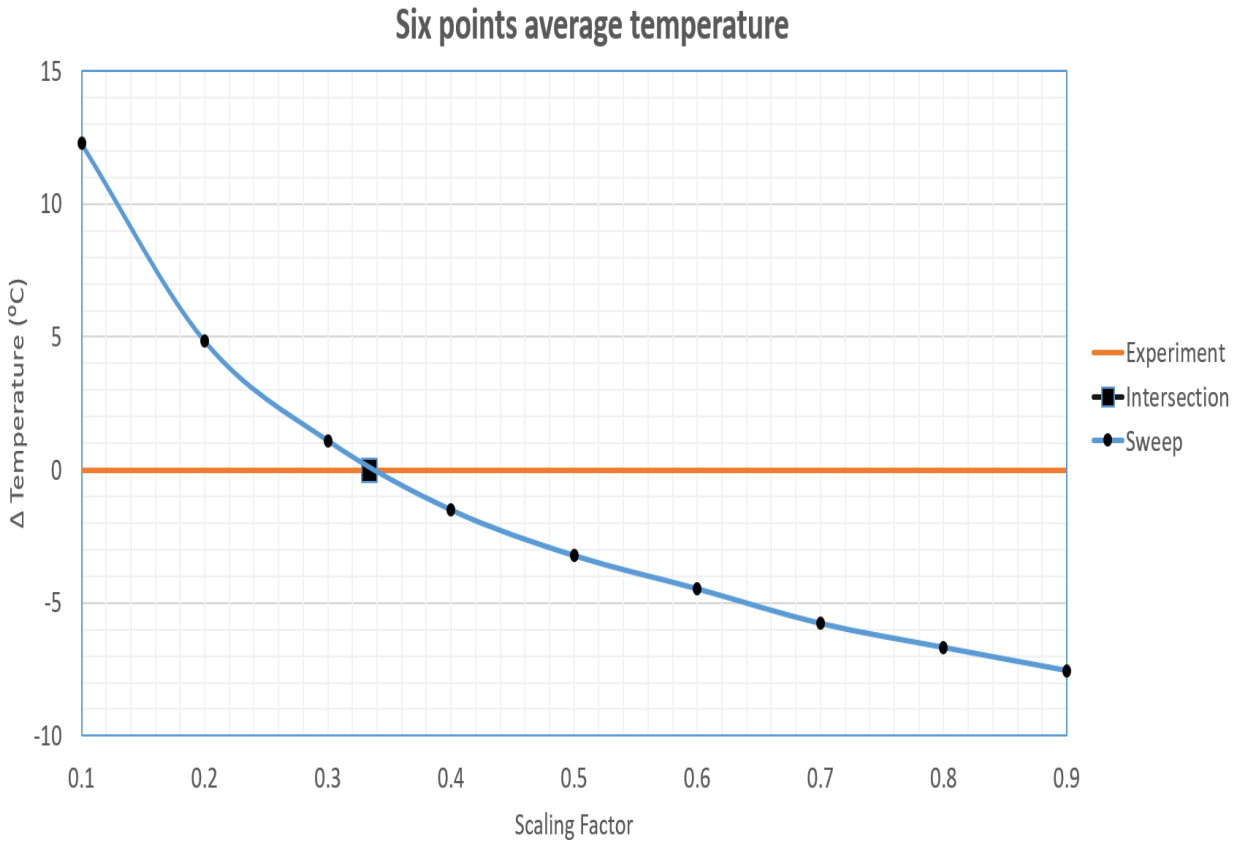

Figure 4.6: *Scaling factor versus six point averaged temperature difference between experiment and simulation*

4.2.2 Convergence

For a steady state simulation, the simulation has been said to be converged if the field values such as temperature and velocity do not change with iterations. Figures 4.7 and 4.8 shows plots of temperature and velocity variation over 10000 iterations. It can be seen that the fluctuations in the points of measurement have flattened out over iterations. The solution does not change very much after 5000 iterations and for this reason all the subsequent simulations was run for 5000 iterations.

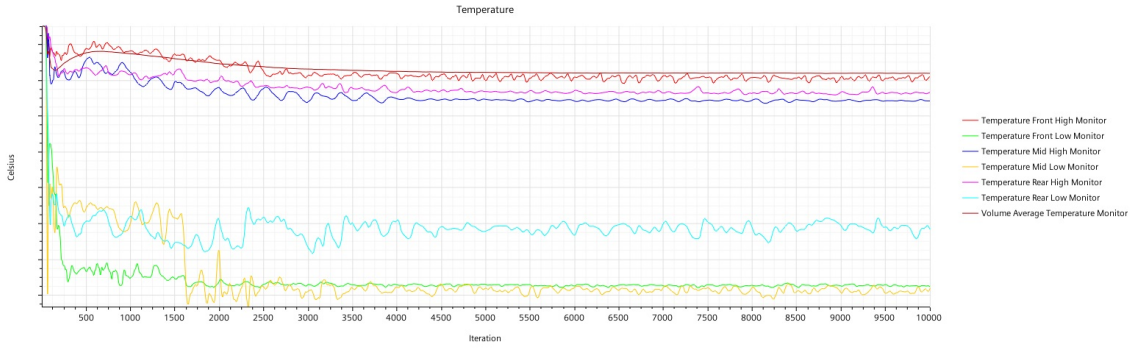

Figure 4.7: *Variation of Temperature at the measured points versus iterations*

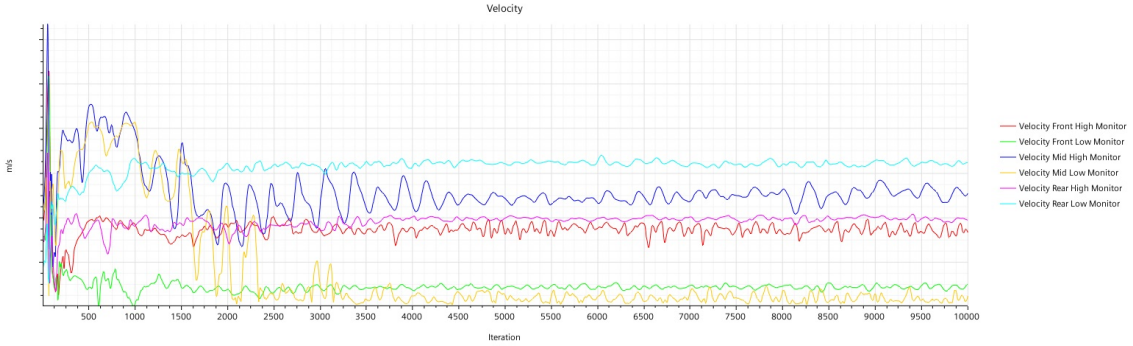

Figure 4.8: *Variation of Velocity at the measured points versus iterations*

It can also be observed that there are very few fluctuations in temperature and velocity over the last 1000 iterations from the figures 4.9 and 4.10. However, a few fluctuations can still be observed and these are removed by averaging. This is done in StarCCM+ by using Field Mean option. A very stable plot of Field mean temperature is shown in figure 4.11 which is used to judge convergence in all the following simulations.

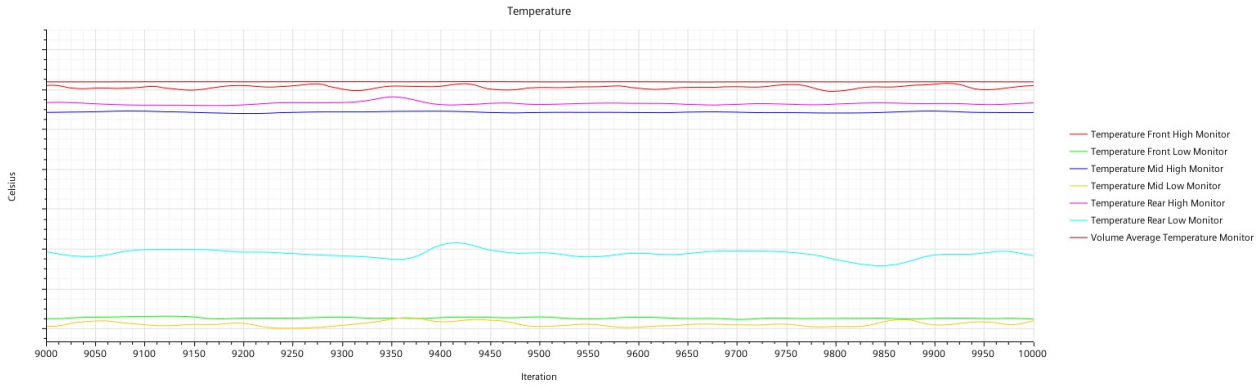

Figure 4.9: *Variation of Temperature at the measured points in the last 1000 iterations*

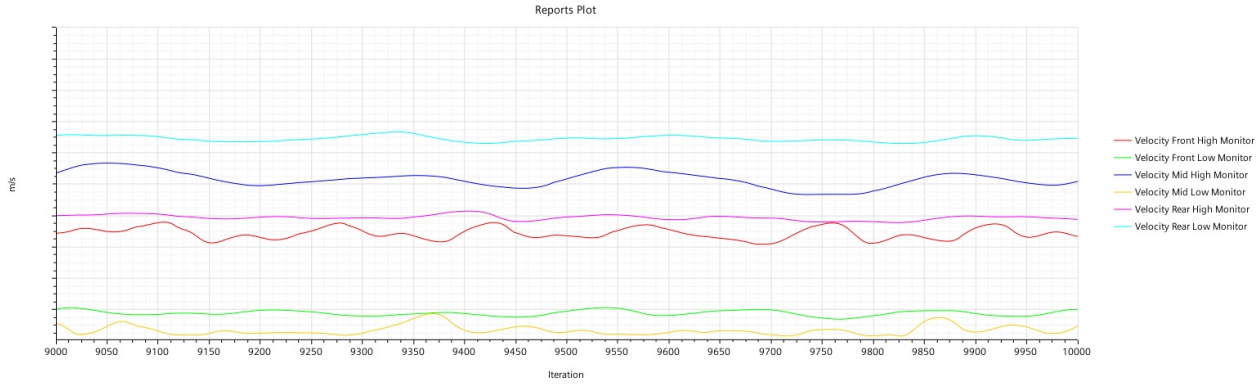

Figure 4.10: *Variation of Velocity at the measured points in the last 1000 iterations*

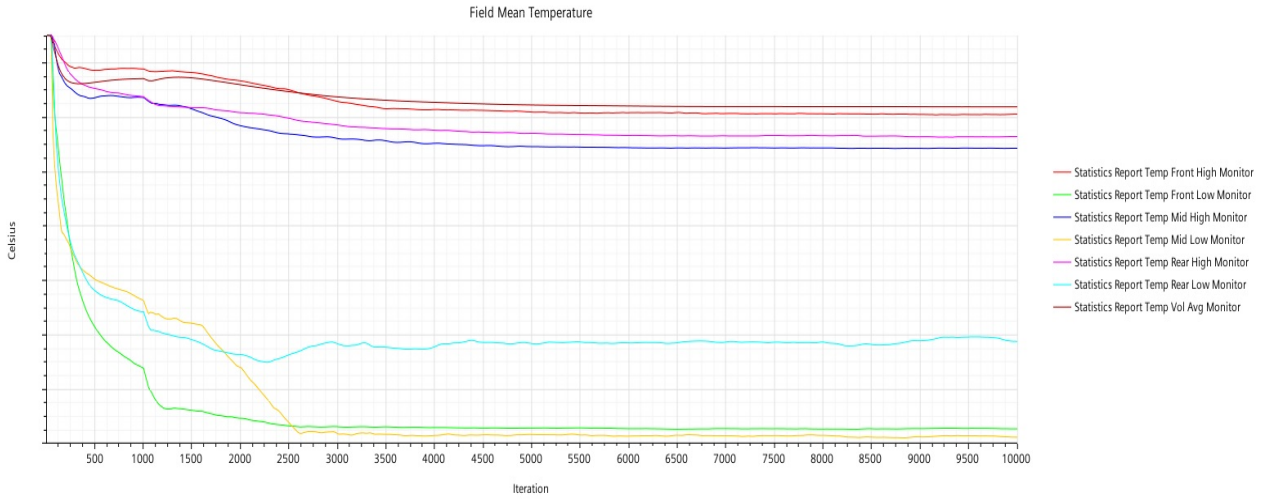

Figure 4.11: *Field mean temperature plot versus iterations*

4.2.3 Flow field

The figures 4.12, 4.13 and 4.14 show the velocity volume render plots in which low velocities are capped out. Figure 4.12 shows clear working of the defroster unit where high velocity flow is pushed out by two fan outlets on to the wind screen. Figure 4.13 shows high velocity blown from the roof unit into the cabin. In figure 4.14 all the flow with more than 0.5 m/s is shown where a stream of air can be seen leaking through the door mechanism of middle door on to the floor.

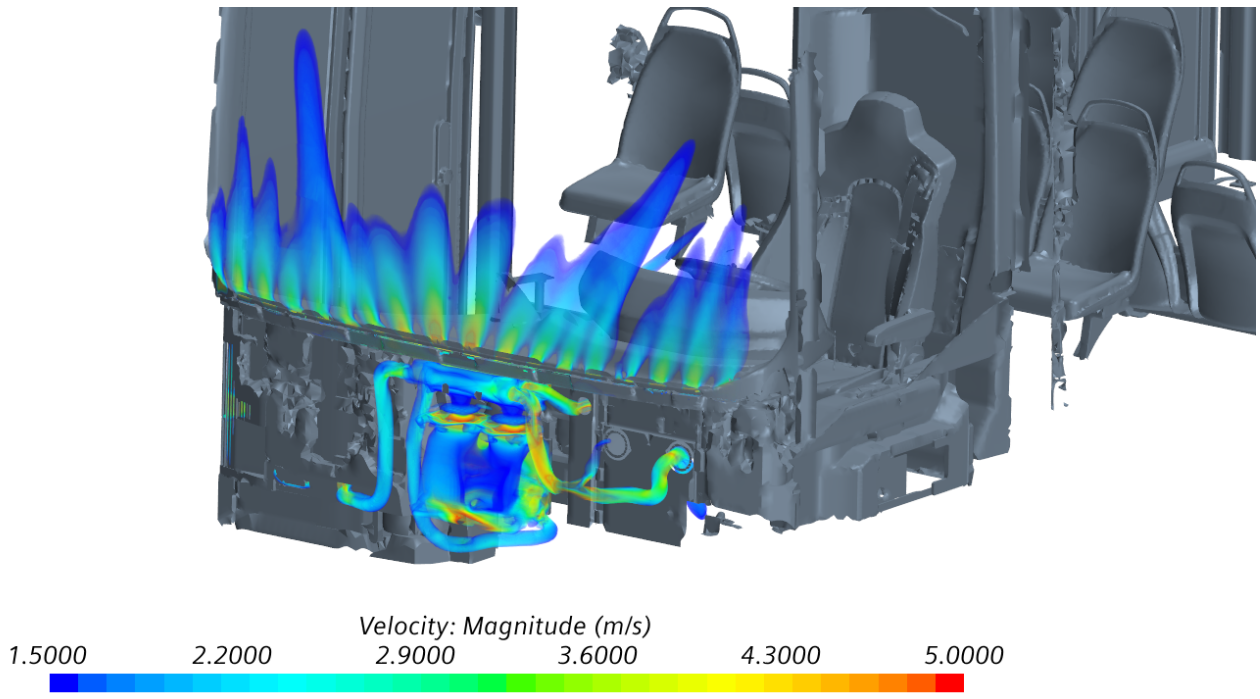

Figure 4.12: *Velocity volume render of flow on the windscreen coming from defroster. High velocities are shown, velocities lower than 1.5 m/s are capped out*

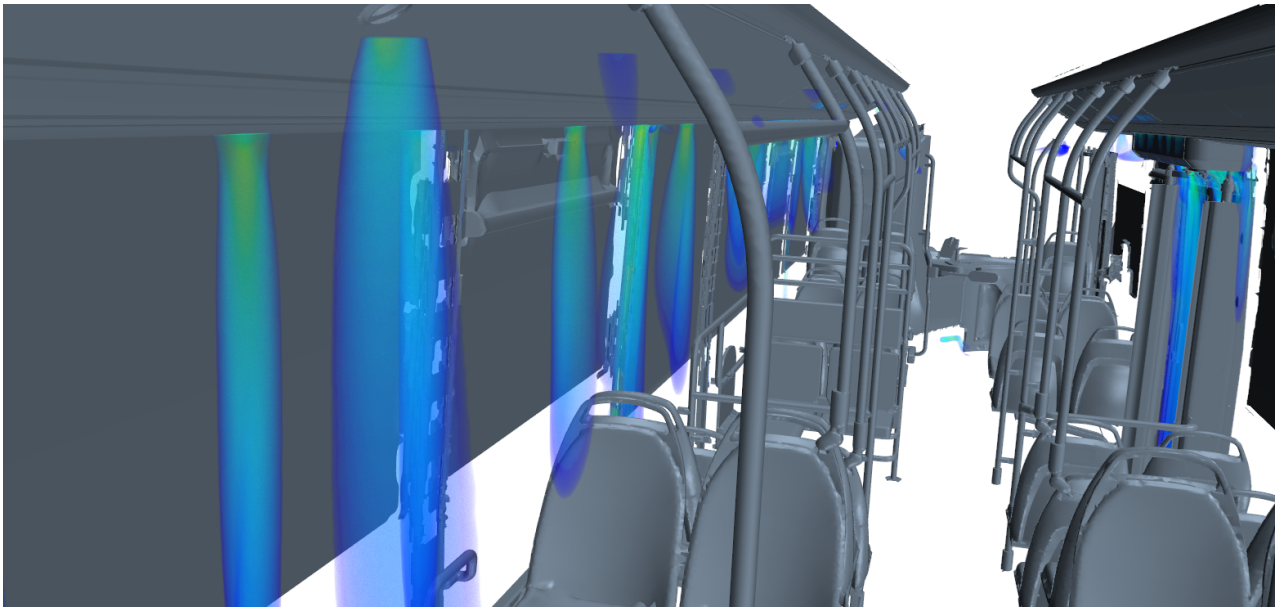

Figure 4.13: *Velocity volume render of flow inside the cabin coming in from air ducts. Colouring scheme shown is with low velocities capped out.*

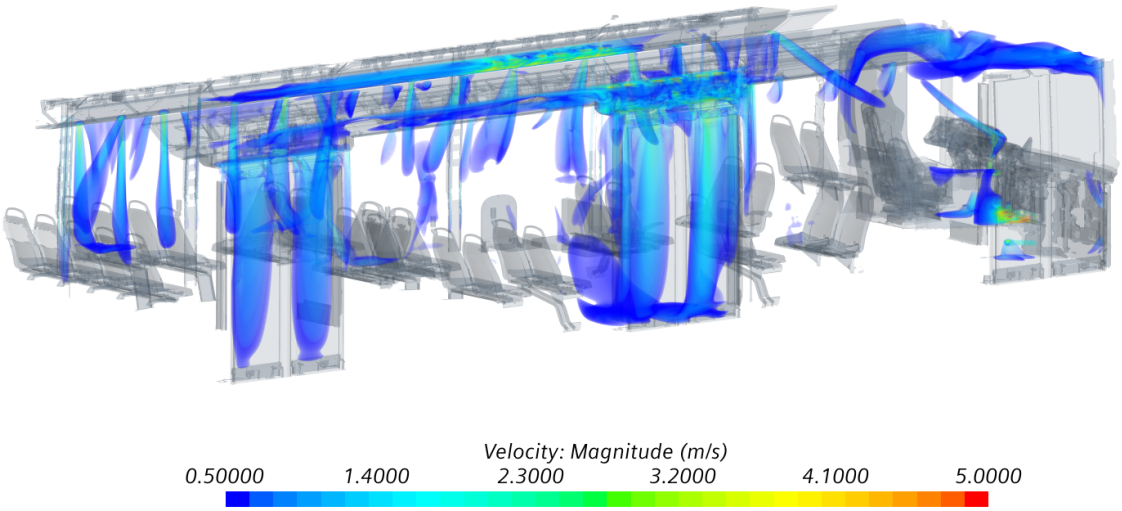

Figure 4.14: *Velocity volume render of full in the whole domain. Colouring scheme shown is with low velocities capped out.*

4.2.4 Temperature distribution

The temperature volume render representing the regions with low temperature in the domain is shown in the figure 4.15. It can observed that almost the entire floor region is covered in this plot with cold air. This is expected as cold air has higher density and it settles at the bottom of the bus. This represents the correct modelling of buoyancy effect. However, a region close to the door is not covered by yellow colour in the plot indicating that it is a region with higher temperature. This is because of the hot air leaking from the roof unit through the door mechanism which was also seen in the figure 4.14.

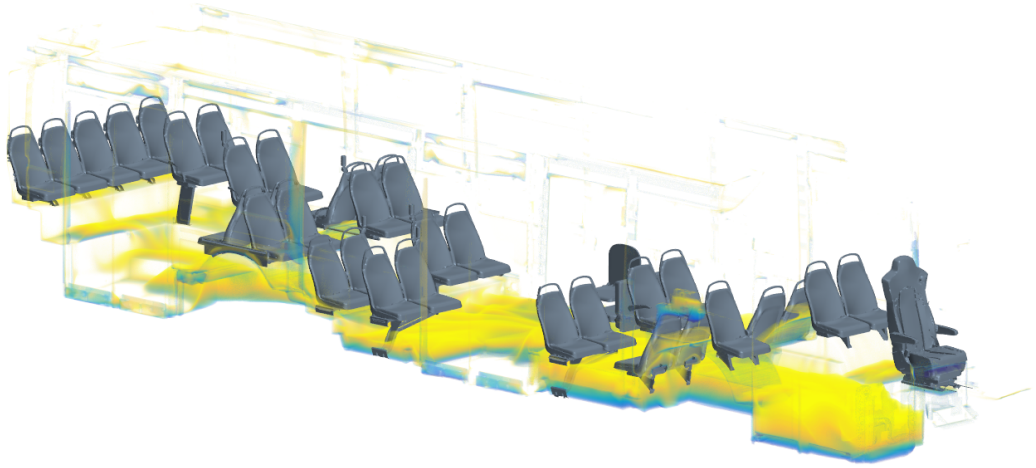

Figure 4.15: *Temperature volume render of full in the whole domain. Colouring scheme shown is by capping out high temperature regions*

4.2.5 Boundary Heat Flux

The figures 4.16 - 4.18 show the plots of heat flux on the boundaries of the domain. Higher value of boundary heat flux represents higher amount of heat transfer through the boundary. In figure 4.16, higher heat flux is observed at the windscreen of the bus. This is because of the hot air leaving from the defroster which helps in de-icing of the windscreen.

Figure 4.17 shows the heat flux across the floor of the bus. Major part of floor shows lower heat flux and this

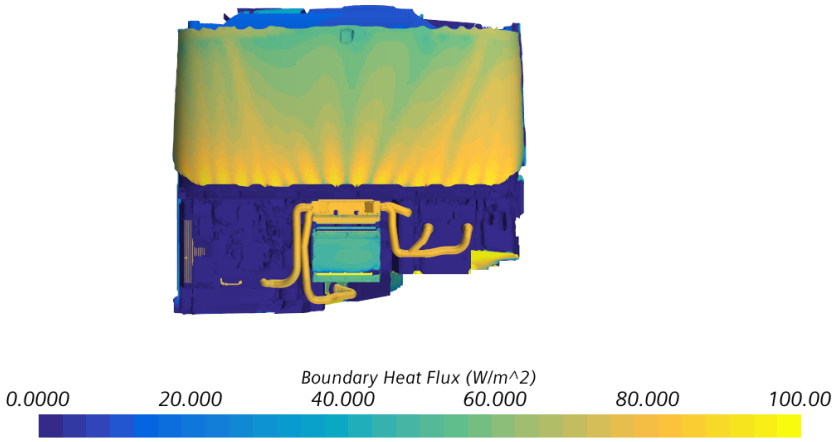

Figure 4.16: *Boundary heat flux plot on windscreen of the bus*

is because of the smaller difference in temperature of cold air settled at the bottom of the bus and ambient air. However, there are some parts of the floor with higher heat flux. This is because of presence of hot air either because of the convectors or due to hot air that is leaked from the roof unit.

Different parts of the bus such as windows, doors, walls, roof and floor show different heat flux values in the figure 4.18. This is because of using different HTC values at these boundaries which is obtained from the U value estimation study[14]. This is more accurate modelling of the heat transfer across the walls of the bus when compared to earlier study made on this bus[10]. This model can now be used to evaluate the effect of changing materials on interior climate for any of these boundaries.

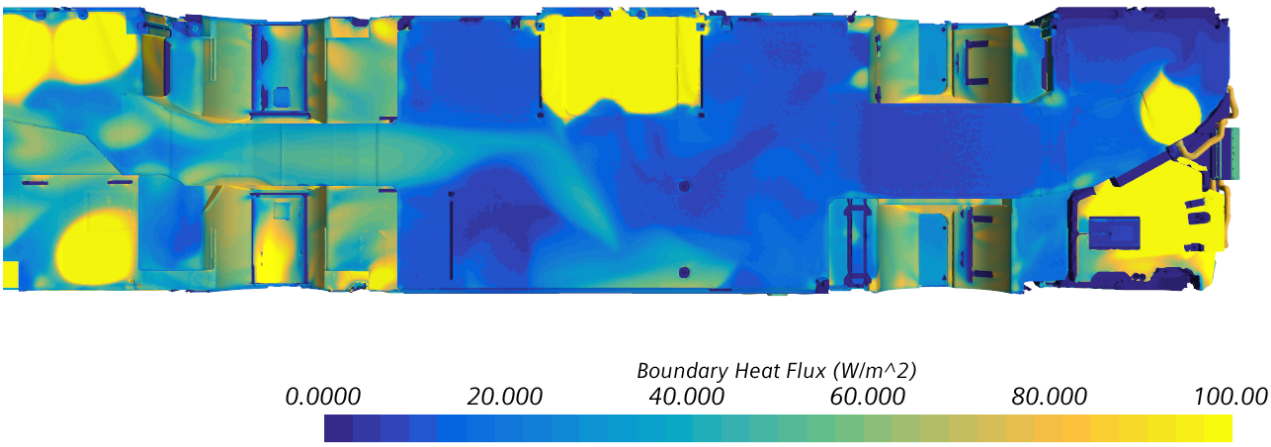

Figure 4.17: *Boundary heat flux plot on floor of the bus*

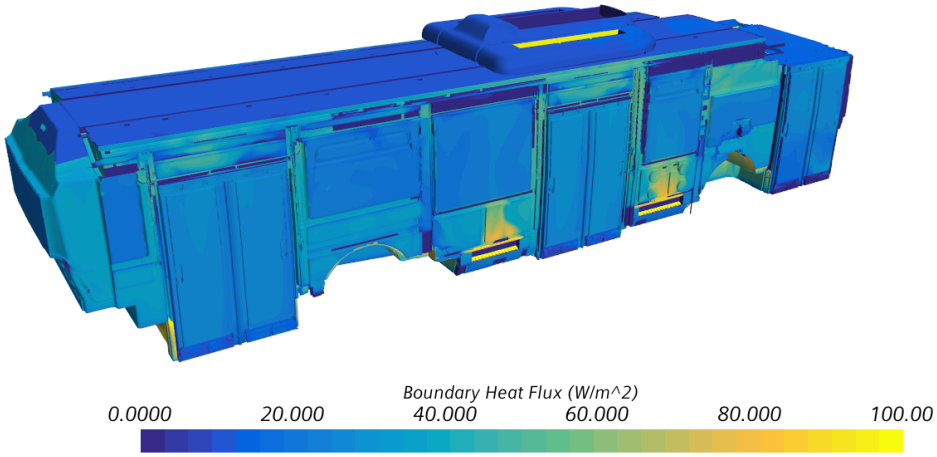

Figure 4.18: *Boundary heat flux plot on walls of the bus*

4.3 Unsteady Model

In this section the results from the unsteady model for the door opening cycle are presented and discussed. The temperature plots shown below have a colouring scheme in which yellow colour indicates hot regions, green colour indicates warm regions and blue colour indicates cold regions.

Initially the unsteady model is run for 4 seconds without any motion of the doors and monitored to make sure that there are no errors are present in the model. Once this was done, the door motion is triggered using the field function for the door regions. The following temperature plots are taken at different time instances to understand the flow and the effect on the interior climate.

Figure 4.19 shows the temperature distribution plots along a plane that is cutting the lower measuring points from the experiments. In this figure it can be observed that the doors open between 4 and 6 seconds. As the doors open cold air rushes into the bus cabin and slowly starts to spread around. The heaters that are present opposite to that of the front and middle doors can be seen working against the entering cold air by spreading heat with the help of a fan. It can also be observed that already at 8 seconds most parts of the bus cabin area in this plane changed colour from green to blue which indicates cold air. At 15 seconds, it is cold everywhere in the plane except areas close to the heaters. Not much is changed in terms of temperature distribution from 15 seconds to 26 seconds in this plane. At 26 seconds of solution time, 20 seconds from the time doors have been completely open, the doors start to close and are completely closed at 28 seconds. If the first picture and the last picture from 4.19 are observed, colour of most parts of the cabin area changes from the green to blue. This shows that the doors opened for 20 seconds is enough time for temperature at the lower plane to drop significantly.

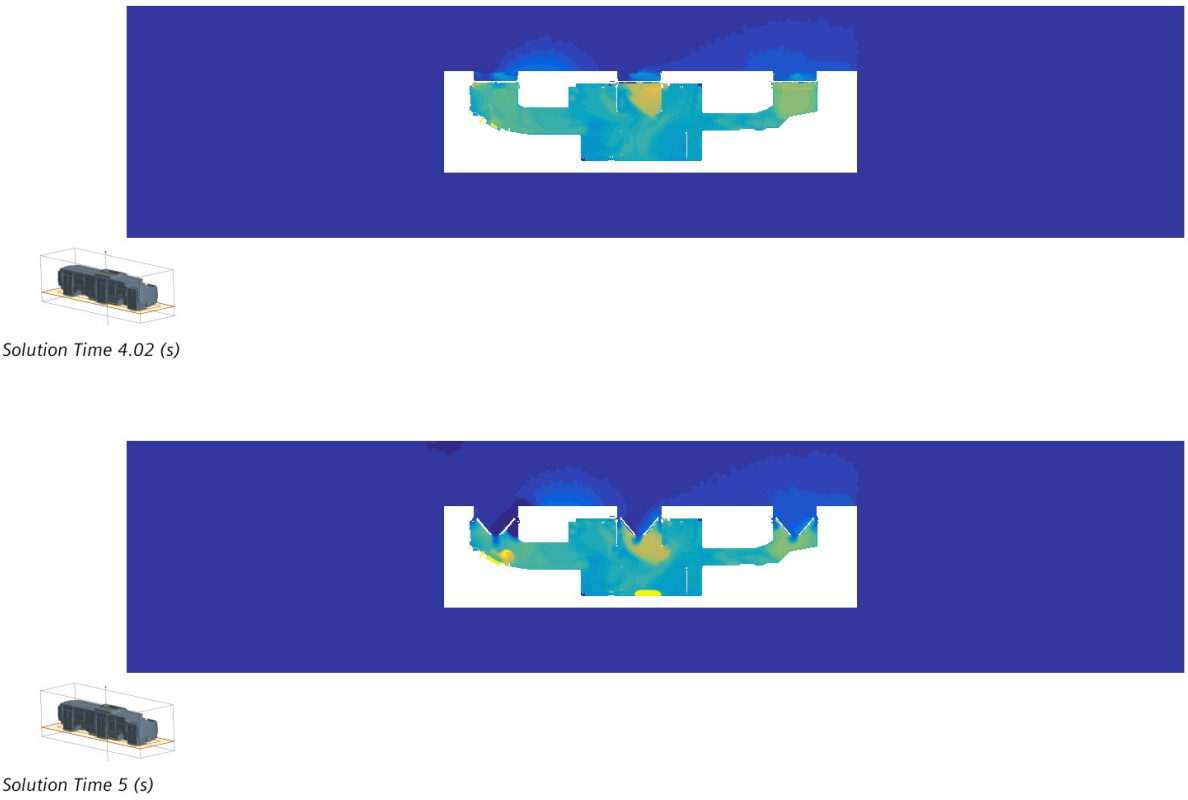

Figure 4.19: *Temperature distribution plot along a plane cutting the lower measuring*

Solution Time 6 (s)

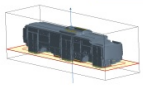

Solution Time 8 (s)

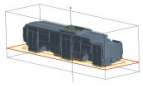

Solution Time 15 (s)

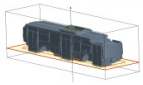

Solution Time 26 (s)

Figure 4.19: *Temperature distribution plot along a plane cutting the lower measuring (cont.)*

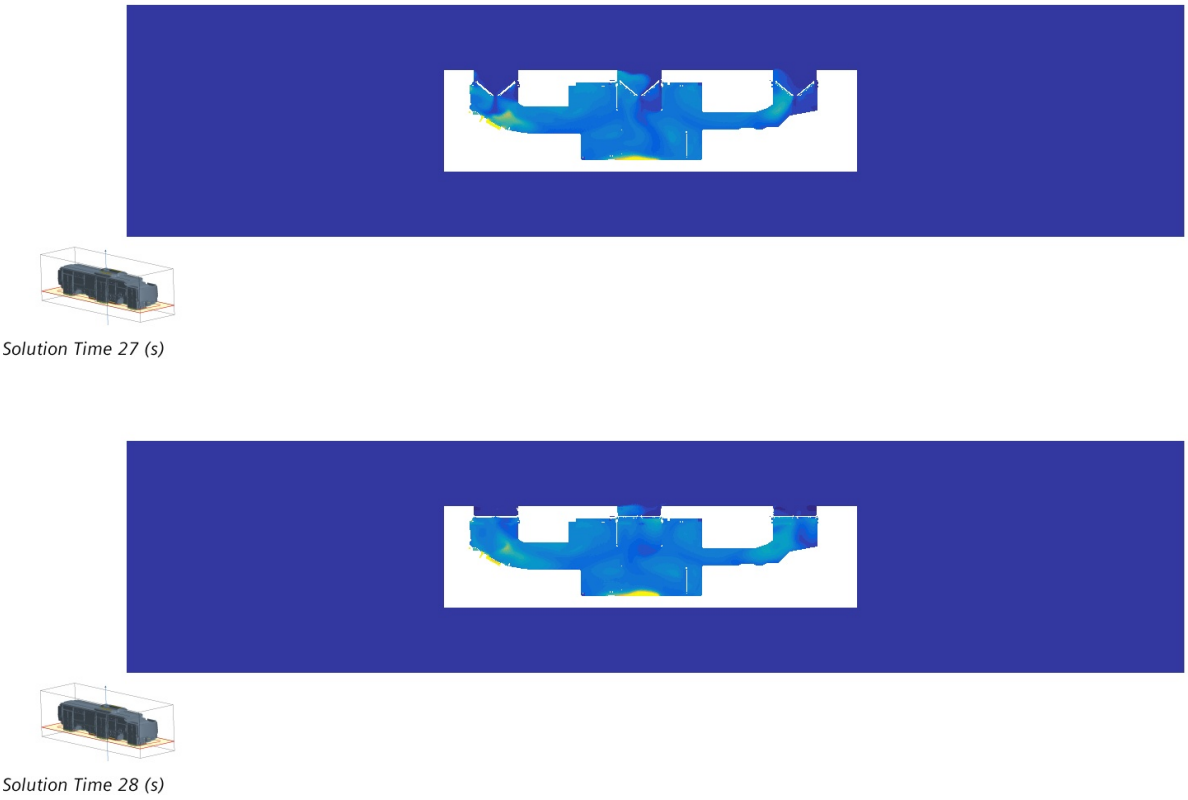

Figure 4.19: *Temperature distribution plot along a plane cutting the lower measuring (cont.)*

Figure 4.20 shows the temperature distribution plots along a plane that is cutting the higher measuring points from the experiments. A similar behavior of cold air entering into the cabin as in case of lower plane is observed when the doors are opened between 4 and 6 seconds, see figure 4.20. At 8 seconds, the cold air starts to spread around the cabin but there are still many areas on this plane which have higher temperature shown in yellow colour. In this figure we can also observe at 15 seconds and 26 seconds the colour of the plot changes from yellow to green and blue indicating drop in temperatures in this plane. Again comparing the first picture of figure and the last picture of figure we can see that there is very big drop in temperatures in this plane as well when the doors are opened for 20 seconds.

It can be observed that in the temperature plots of figure 4.19 the temperature distribution in the climate chamber is undisturbed. However, in the temperature plots of figure 4.20, temperature distribution is disturbed close to the doors in the climate chamber. This gives a clear idea on the movement of air when the doors are open. On lower parts of the bus, cold air enters the cabin and on the higher parts of the bus some amount hot air escapes the bus volume.

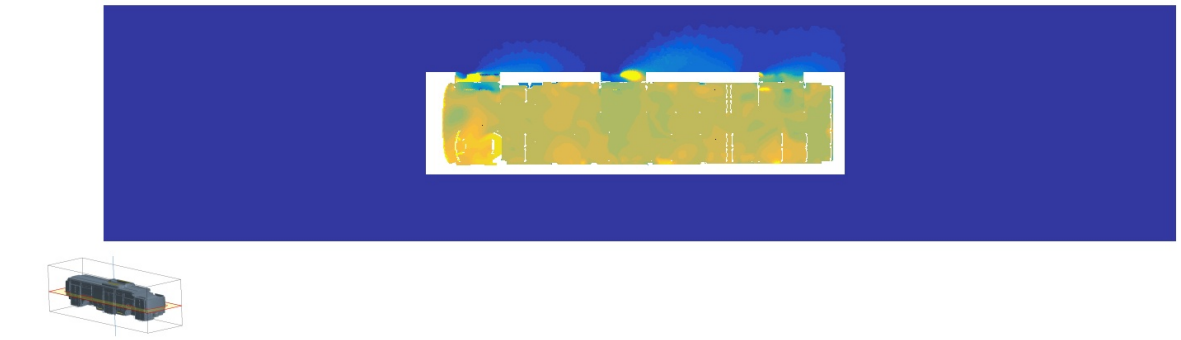

Solution Time 4.02 (s)

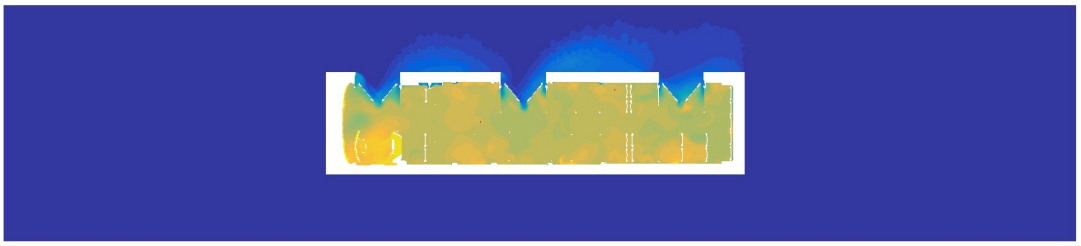

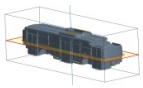

Solution Time 5 (s)

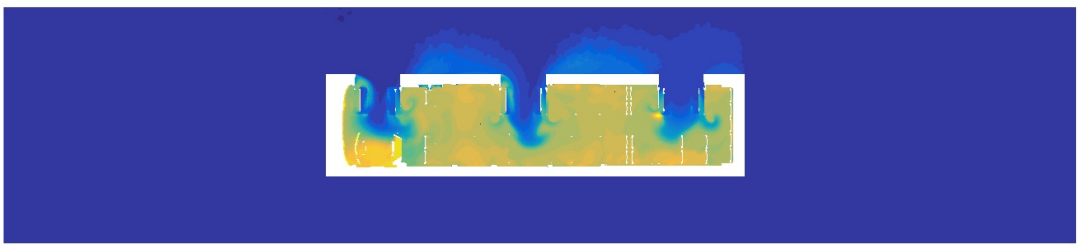

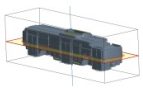

Solution Time 6 (s)

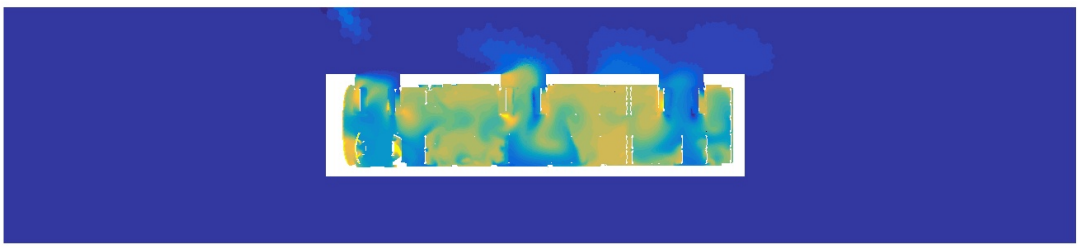

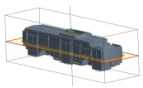

Solution Time 8 (s)

Figure 4.20: *Temperature distribution plot along a plane cutting the higher measuring points*

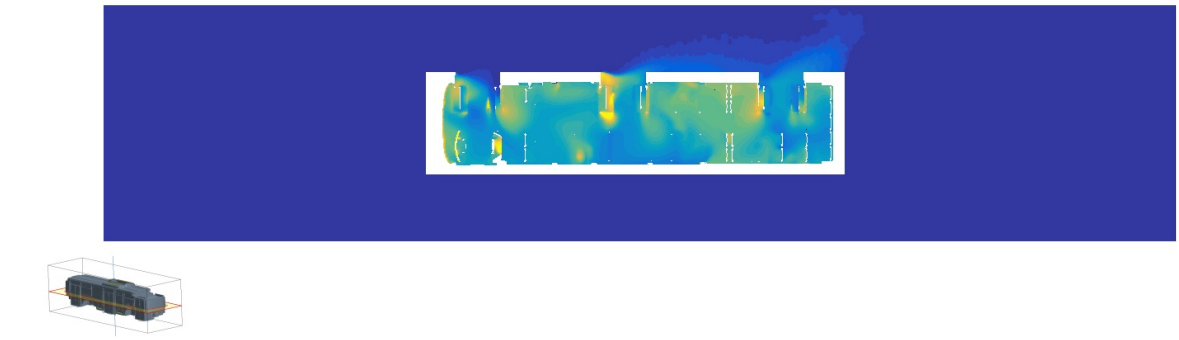

Solution Time 15 (s)

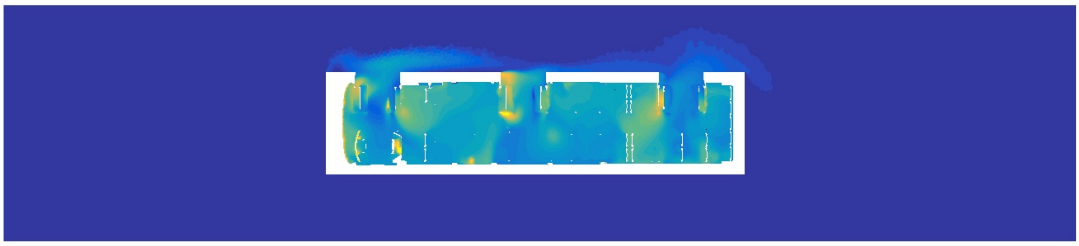

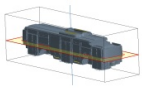

Solution Time 26 (s)

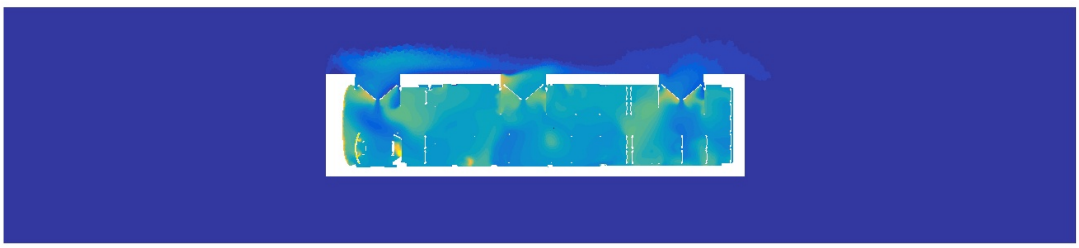

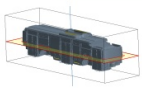

Solution Time 27 (s)

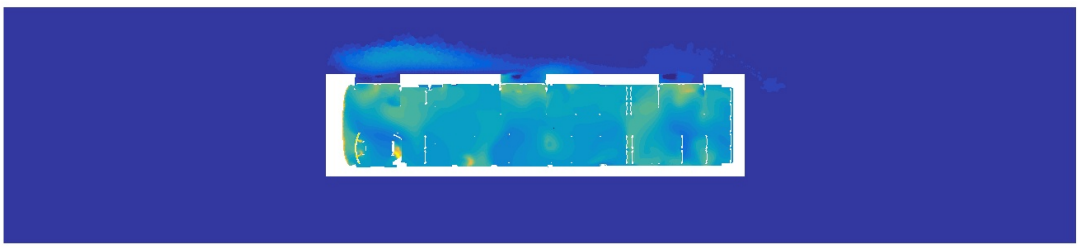

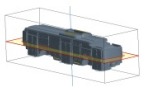

Solution Time 28 (s)

Figure 4.20: *Temperature distribution plot along a plane cutting the higher measuring points (cont.)*

The movement of air can be understood using the temperature distribution figure 4.21 plotted along the width of the bus at the front door. In this figure we can see how the cold air entering the cabin pushes hot air inside against the walls of the bus at solution time of 6 seconds. When the time is marched on till 8 seconds, we can see the cold air settling at the bottom of the bus and hot air occupying the upper parts of the bus. After this we can see the hot regions slowly disappearing in the pictures shown for 15 and 26 seconds of solution which suggests that the hot air leaves the bus volume through the top part of the opening. The entry for cold air is stopped when the doors are completely closed which can be seen in the plot made at 28 seconds of solution in figure 4.21.

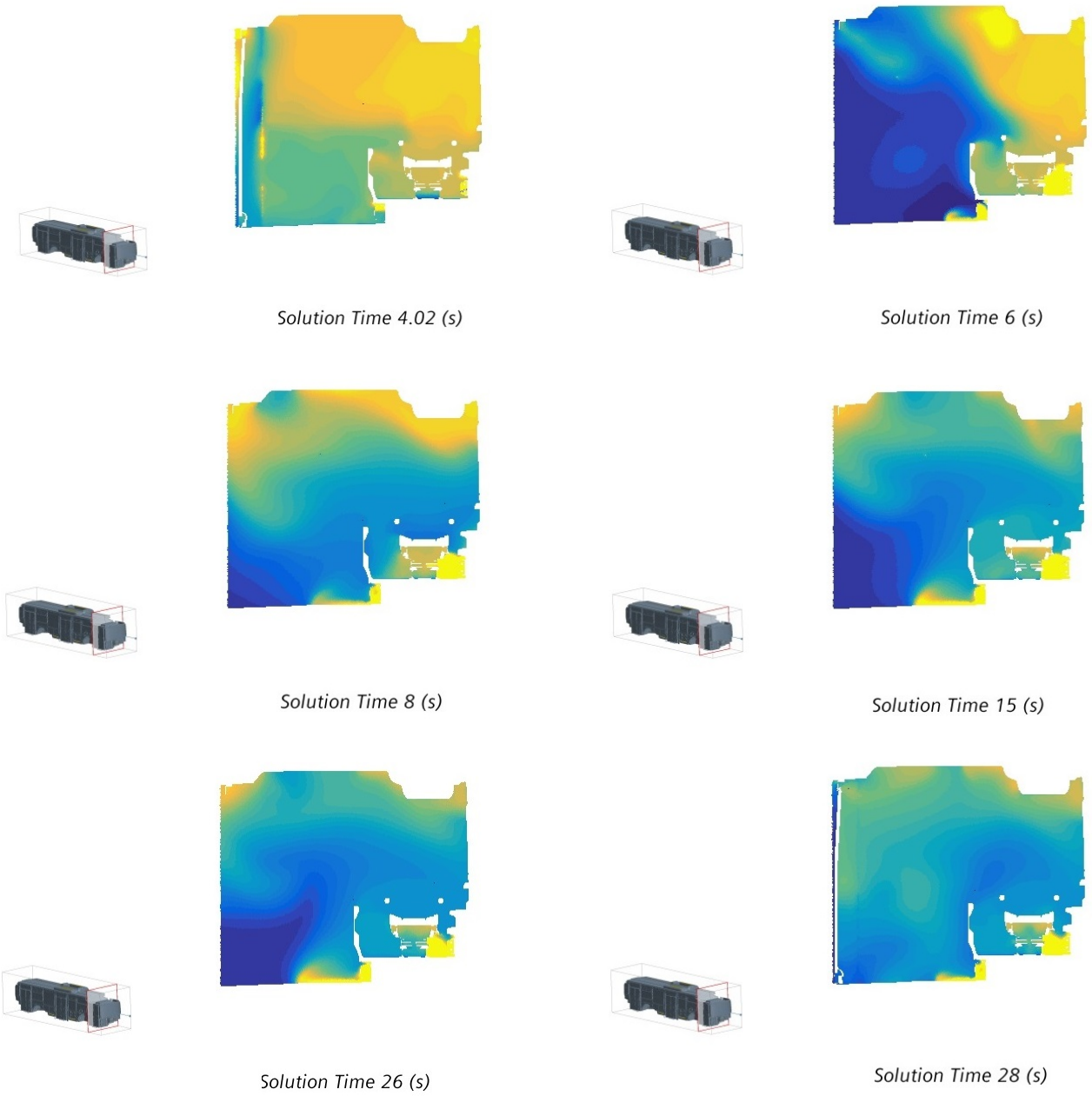

Figure 4.21: *Temperature distribution plot along a plane at the middle of the front door*

Once the doors have closed at 28 seconds, the simulation is run for another 2 minutes to complete the standard door opening cycle. Figures 4.22 and 4.23 show temperature distribution on lower and higher planes respectively at different time instances after the doors are closed. In figure 4.22 we can see that there is no significant change in temperature distribution during this 2 minutes. Hot air is spread around by the heaters but still large amount of area in this plane is cold. If the last picture in this plot is compared to the first picture of the figure 4.19 we can see the temperature drop in this plane because of opening and closing the doors.

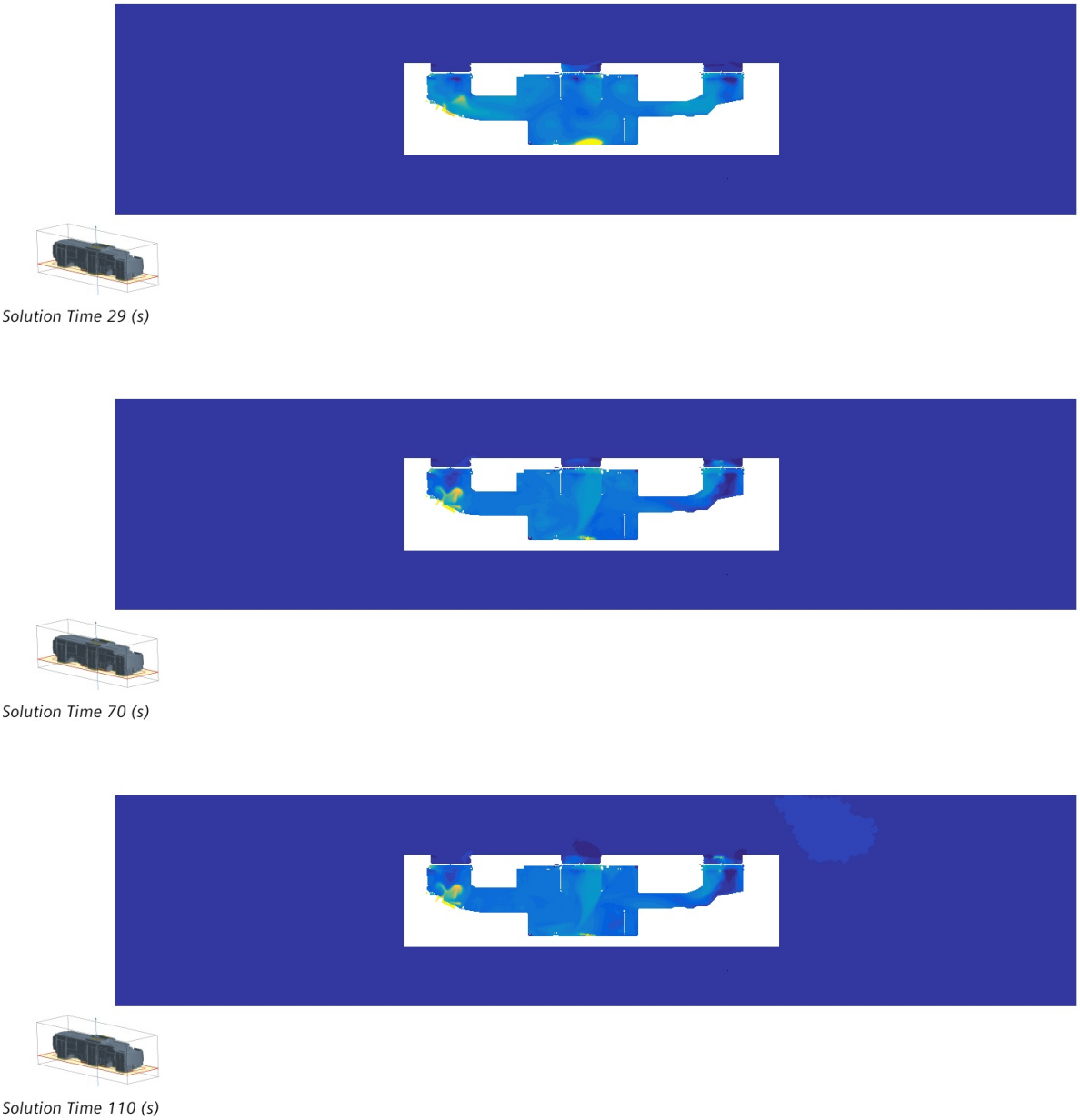

Figure 4.22: *Temperature distribution plot along a plane cutting the lower measuring points after the doors are closed*

Solution Time 148 (s)

Figure 4.22: *Temperature distribution plot along a plane cutting the lower measuring points after the doors are closed (cont.)*

In figure 4.23 we can see some change in temperature distribution from 29 seconds to 148 seconds of solution time. Blue areas have changed to green colour at the end of two minutes indicating that higher parts of the bus is getting warmer with time. However if the last picture in this plot is compared to the first picture of the figure 4.20 we can see that the colour of the bus region is changed from yellow to green indicating a net temperature drop due the door opening cycle.

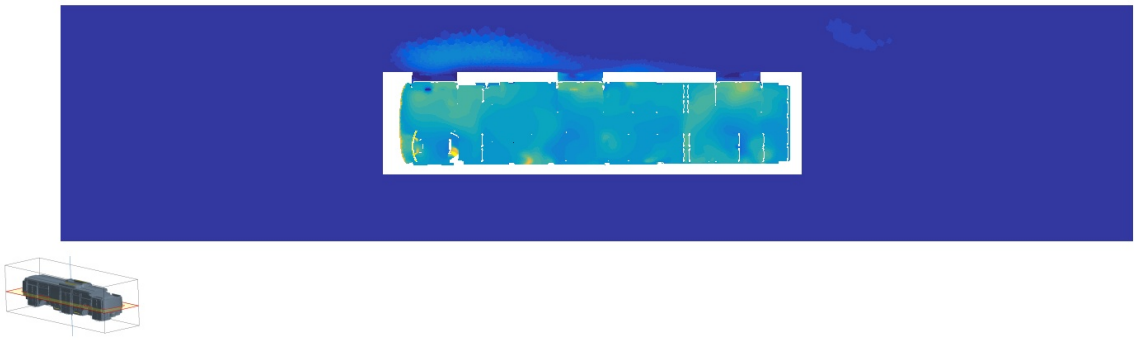

Solution Time 29 (s)

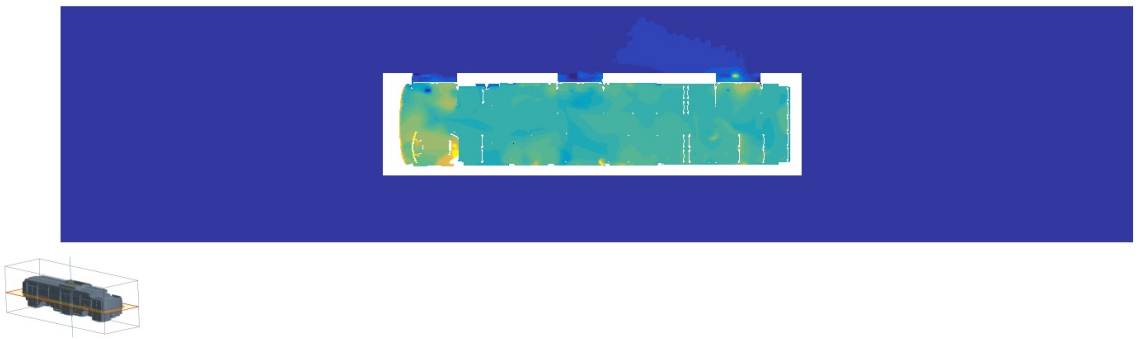

Solution Time 70 (s)

Figure 4.23: *Temperature distribution plot along a plane cutting the higher measuring points after the doors are closed*

Solution Time 110 (s)

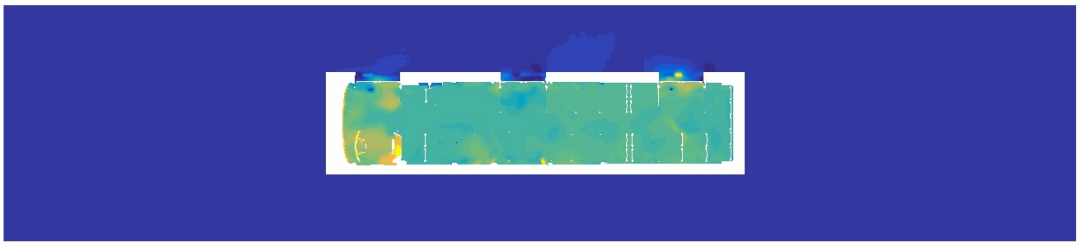

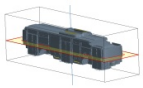

Solution Time 148 (s)

Figure 4.23: *Temperature distribution plot along a plane cutting the higher measuring points after the doors are closed (cont.)*

The results of temperature variation throughout the door opening cycle can be summarised using the plot 4.24. The first four seconds of the simulation when there is no motion of doors, the temperature do not change from the initial steady state values. When the doors are opened at 4 seconds, there is drop in temperature at all the six points. The upper and lower measuring points show small increase in temperature at around 8 seconds. This is the point in time at which the cold air that entered the bus volume starts to settle at the bottom and hot air occupy the upper regions as seen in figure 4.21. This mixing of cold and hot air is the reason for the increase in temperature at the measuring points. The temperature of the upper measuring points further drop after 10 seconds until the doors are completely closed. This is due to the hot air leaving from the top region of the bus. The lower measuring points show similar temperature from 10 seconds to 26 seconds which indicates that there is very little movement of air at the bottom of the bus in this instance. After the doors are closed at 28 seconds, the upper measuring points slowly starts to increase in temperature all the way up to the end of the door cycle. However, the temperatures at the lower measuring points continue to remain low for the rest of the door cycle. This was also seen in the figures 4.22 and 4.23.

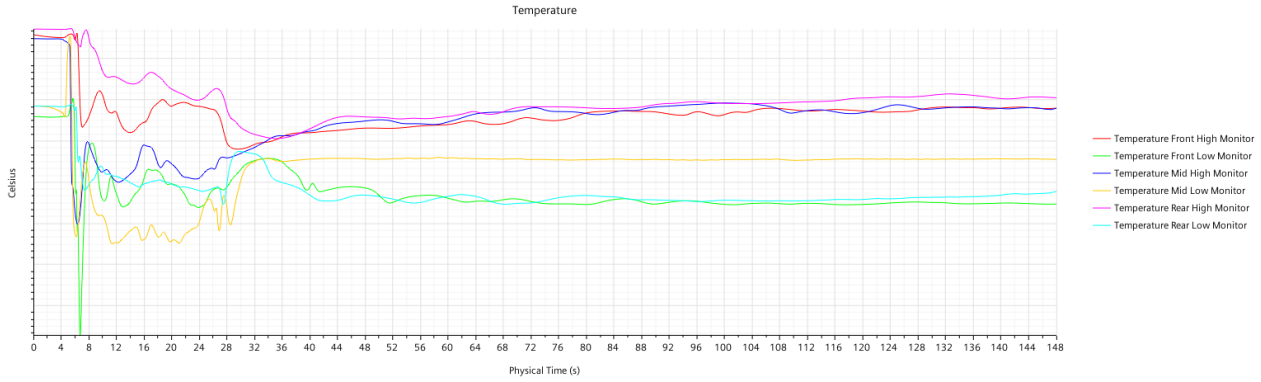

Figure 4.24: *Temperature versus time for the whole door opening cycle*

5

Conclusions

In this study a methodology for simulating the interior climate of an electric bus was established for a steady state case and unsteady state case. The major outcomes are discussed in this chapter.

It was found that it is important to have a good mesh to have a stable solution. A good mesh starts with a good surface mesh. Surface wrapper along with surface remesher in StarCCM+ is used in this thesis to define the volume of interest by removing unnecessary components and to provide good surface mesh. The volume mesh was then refined until the solution was stable.

The boundary conditions specified at different HVAC components and at the walls of the bus defines the steady state model. The results from the final steady state model shows correct working of all the components of HVAC system with realistic flow field. However, the heat released at the convectors and heaters are taken from the ideal manufacturer data. This data should be measured on the bus to make the steady state model more accurate.

To model the heat transfer through the walls of the bus, a scaling factor is multiplied with the initial values of HTC and swept through a range of values until the temperatures inside the bus match the experimental values. This way the model is calibrated with the experimental data to get a realistic model for considered case of -8.3°C. To simulate other climate conditions, the model has to be calibrated with corresponding experimental data after making the necessary changes to the boundary conditions.

This calibrated steady state model can be used to evaluate the effect on interior climate when a material of part is changed. To see such effects the heat transfer through conduction value(initial HTC value) should be calculated and then multiplied with the calibrated scaling factor which is then set as HTC at that particular boundary. This way the current model can be used in the process of selecting materials for any exterior part of the bus.

The calibrated model is then converted into an unsteady model to simulate the door opening cycle. The door opening cycle that is simulated is with 20 seconds of opened doors followed by 2 minutes of closed doors simulation. The motion of doors while opening and closing was obtained by overset mesh methodology. Solution from steady state simulation is used as an initial condition for this case.

When the doors were opened for 20 seconds it was observed that the cold air rushes into the bus volume and the temperatures dropped significantly everywhere inside the bus. The heaters started to spread heat but its effect was restricted to close surroundings. After the doors closed, simulation was run for 2 minutes to find that the bottom parts of the bus continue to be cold and the temperature on top parts of the bus increase slightly. However, temperature inside the bus significantly dropped when compared to the temperature before opening the doors. This signifies the total loss in energy because of the door opening cycle and reiterates the need for a solution to reduce these loses.

This model can be used to evaluate solutions that are designed to counter the losses in the system. This model can also be used to evaluate the losses with other door opening cycles.

The boundary conditions specified for the unsteady model are constant in time. The time dependent heat output data for the convectors, heaters and other heat exchangers is necessary to make the current model more accurate. Temperature and flow field data measured from the experiments for the door opening cycle are necessary to validate the model.

Bibliography

[1] Jenkins, P.L., Phillips, T.J., Mulberg, E.J. and Hui, S.P., 1992. Activity patterns of Californians: use of and proximity to indoor pollutant sources. Atmospheric Environment. Part A. General Topics, 26(12), pp.2141-2148.

[2] Velt, K.B. and Daanen, H.A.M., 2017. Optimal bus temperature for thermal comfort during a cool day. Applied ergonomics, 62, pp.72-76.

[3] Zhang, H., Dai, L., Xu, G., Li, Y., Chen, W. and Tao, W.Q., 2009. Studies of air-flow and temperature fields inside a passenger compartment for improving thermal comfort and saving energy. Part I: Test/numerical model and validation. Applied Thermal Engineering, 29(10), pp.2022-2027.

[4] Zhang, H., Dai, L., Xu, G., Li, Y., Chen, W. and Tao, W., 2009. Studies of air-flow and temperature fields inside a passenger compartment for improving thermal comfort and saving energy. Part II: Simulation results and discussion. Applied Thermal Engineering, 29(10), pp.2028-2036.

[5] Liebers, M., Tretsiak, D., Klement, S., Bäker, B. and Wiemann, P., 2017. Using Air Walls for the Reduction of Open-Door Heat Losses in Buses. SAE International Journal of Commercial Vehicles, 10(2017-01-9179), pp.423-433.

[6] de Lieto Vollaro, R., 2013. Indoor climate analysis for urban mobility buses: a CFD model for the evaluation of thermal comfort. Int. J. Environ. Prot. Policy, 1, pp.1-8.

[7] EKICI, Ö. and Güney, G., 2017. Experimental And Numerical Investigations Of Heating In A Bus Cabin Under Transient State Conditions. WIT Transactions on Engineering Sciences, 118, pp.49-59.

[8] Suárez, C., Iranzo, A., Salva, J.A., Tapia, E., Barea, G. and Guerra, J., 2017. Parametric investigation using computational fluid dynamics of the HVAC air distribution in a railway vehicle for representative weather and operating conditions. Energies, 10(8), p.1074.

[9] Dygert, R.K. and Dang, T.Q., 2010. Mitigation of cross-contamination in an aircraft cabin via localized exhaust. Building and Environment, 45(9), pp.2015-2026.

[10] Johansson, E.E. and Skärby, M., 2019. Interior climate simulation of electric buses.

[11] L. Davidson, Fluid mechanics, turbulent flow and turbulence modeling. Chalmers University of Technology.

[12] Siemens, Star CCM+ User Guide. Version 2020.1

[13] Siemens, The Steve Portal, Guidelines for Star CCM+ by Siemens, https://thesteveportal.plm.automation.siemens.com/

[14] Sahraei, H., 2020. Interior Climate U-Value calculation and optimization for electric buses at Volvo buses.